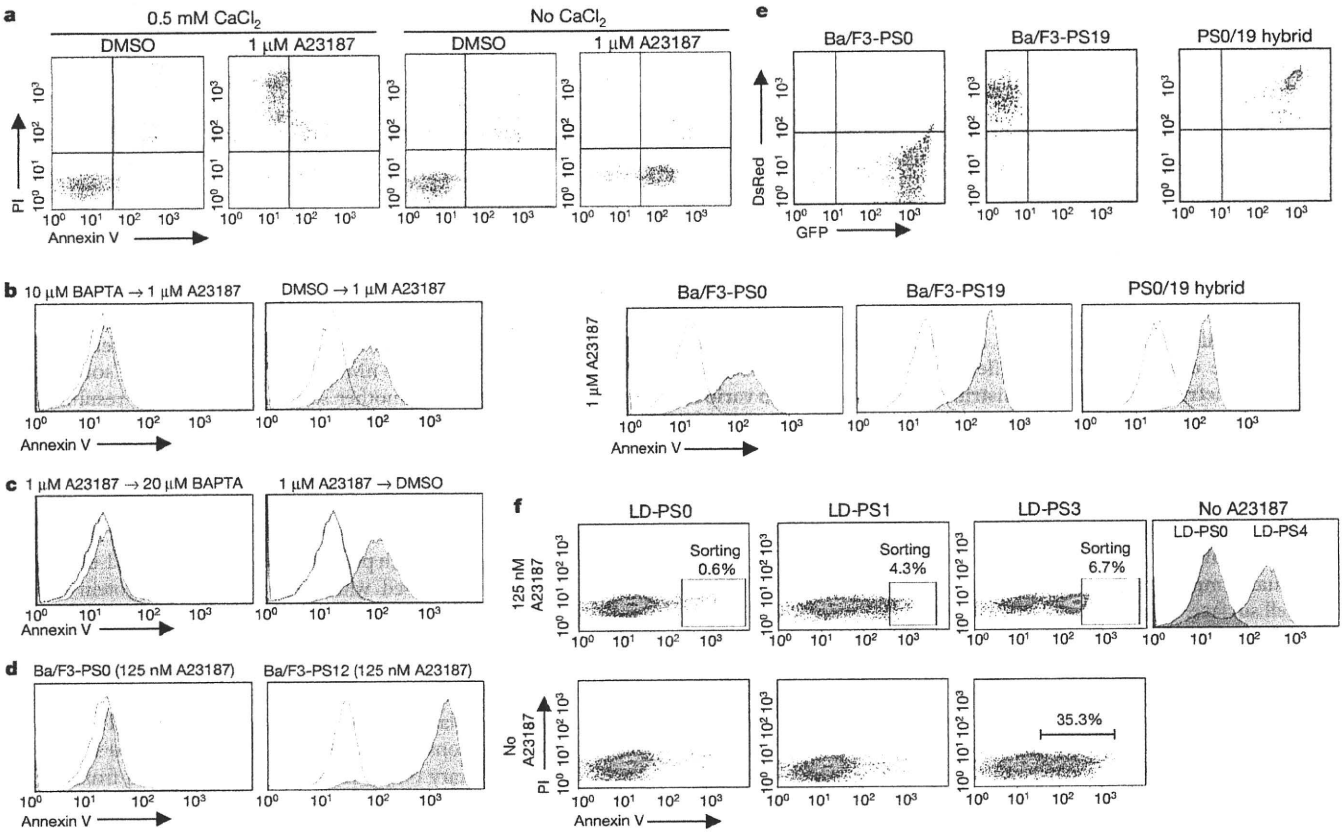

Figure 1 | Molecular cloning of TMEM16F. **a**, Ba/F3 cells were treated with A23187 with or without $CaCl_2$, and stained with Annexin V and PI. DMSO, dimethylsulphoxide. **b**, Ba/F3 cells were incubated with BAPTA-AM and treated with A23187. An Annexin V profile in a PI-negative population is shown. Open curve, profile of resting cells. **c**, Ba/F3 cells were treated with A23187 and then with BAPTA-AM for 5 min, and stained with Annexin V. **d**, Ba/F3 cells and cells after sorting for 12 cycles (PS12) were treated with A23187 and stained with Annexin V. **e**, GFP and DsRed profiles of PS0, PS19 and PS0/19 hybrid cells are shown. Bottom: the same cells were treated with A23187 and stained with Annexin V. **f**, Ba/F3 cells transformed with PS19 cDNA library were treated with A23187, stained with Annexin V and sorted (LD-PS0). Annexin V and PI profiles of cells after first (LD-PS1) and third (LD-PS3) sorting are shown. Right: Annexin V profile of original cells (LD-PS0) and after fourth sorting (LD-PS4) without A23187.

Ba/F3 cells (Fig. 2e). The intracellular Ca^{2+} concentration and the kinetics of the Ca^{2+} influx after treatment with A23187 was similar among the vector-transformed cells and those expressing wild-type and D409G mutant TMEM16F (Supplementary Fig. 2). These results indicated that TMEM16F mediates a Ca^{2+}-dependent scramblase activity for PtdSer, and that its D409G mutant is sensitized to respond to the normal intracellular concentration of Ca^{2+} to expose PtdSer.

Phospholipid scramblase mediates the bidirectional transfer between plasma membrane leaflets of all phospholipids. Cells expressing the D409G mutant TMEM16F were stained with Ro09-0198 (Supplementary Fig. 3a), a tetracyclic polypeptide that specifically binds phosphatidylethanolamine (PtdEtn)[17], indicating that they constitutively exposed PtdEtn, a phospholipid that, like PtdSer, is normally sequestered to the inner leaflet. Treatment of Ba/F3 cells with A23187 caused exposure of PtdEtn. This process was accelerated by overexpressing wild-type TMEM16F (Supplementary Fig. 3b). When 1-oleoyl-2-{6-[(7-nitro-2-1,3-benzoxadiazol-4-yl)amino]hexanoyl}-*sn*-glycero-3-phosphocholine (NBD-PtdCho) was added to the culture, it was quickly internalized by the D409G-mutant-expressing cells (Fig. 2f): of the cell-associated NBD-PtdCho, more than 40% became resistant to extraction with BSA within 6 min. When the cells expressing wild-type TMEM16F were treated with A23187, they incorporated NBD-PtdCho faster than the parental cells, and about 40% of the cell-associated NBD-PtdCho was inside the cells within 4 min (Fig. 2g). Similar results—that is, constitutive internalization by cells expressing the mutant TMEM16F, and enhanced A23817-induced incorporation by cells expressing wild-type TMEM16F—were obtained with *N*-{6-[(7-nitro-2-1,3-benzoxadiazol-4-yl)amino]hexanoyl}-sphingosine-1-phosphocholine (NBD-SM) (Supplementary Fig. 4). The internalized NBD-PtdCho and NBD-SM were intact (Supplementary Fig. 5). Dynasore, which inhibits dynamin-mediated endocytosis[18] inhibited the internalization of these phospholipids only slightly or not at all (Supplementary Fig. 6), suggesting that the contribution of endocytosis to TMEM16F-mediated phospholipid internalization may not be great.

Expression of endogenous TMEM16F in Ba/F3 cells was then knocked down by expressing *Tmem16f* short hairpin RNA (shRNA). As shown in Fig. 3a and Supplementary Fig. 7, the expression level of *Tmem16f* messenger RNA in five transformants was decreased to 20–35% of that in the cells expressing the control shRNA. The rate of A23187-induced exposure of PtdSer and PtdEtn was decreased in these transformants (Fig. 3b, c). Similarly, the uptake of NBD-PtdCho and NBD-SM was slower in *Tmem16f* shRNA-transformed cells (Fig. 3d, e).

Platelets and other blood cells from patients with Scott syndrome show a defect in their ability to expose PtdSer in response to a Ca^{2+} ionophore[7,19]. B-cell lines have been established from a patient with Scott syndrome and from the patient's parents[20]. In agreement with previous reports[8,20], the patient-derived cells did not expose PtdSer in response to a Ca^{2+} ionophore (Fig. 4a). In contrast, A23187 elicited PtdSer exposure in cell lines derived from the patient's parents at the same levels as in cell lines from healthy volunteers. An RT–PCR analysis of the *TMEM16F* mRNA (GenBank accession number NM_001025356) showed that the 5′ part (1,320 base pairs (bp)), corresponding to exons

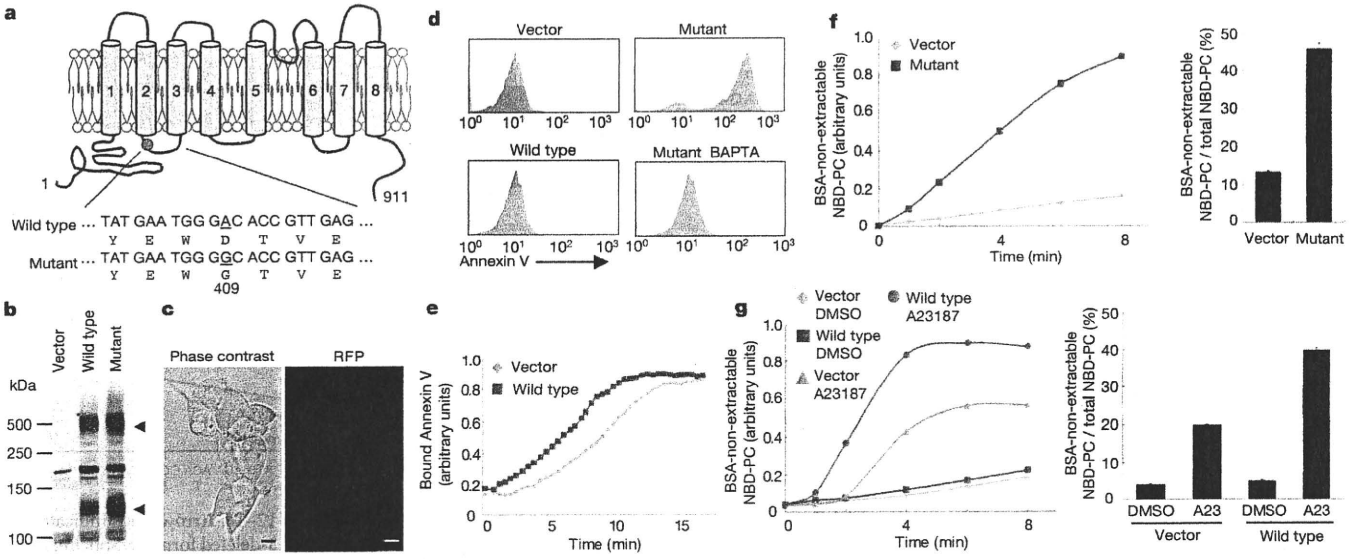

Figure 2 | Phospholipid scrambling in TMEM16F-expressing cells. **a**, Schematic representation of mouse TMEM16F and D409G mutant. **b**, Western blotting of Ba/F3 cells expressing Flag-tagged wild-type and mutant TMEM16F with anti-Flag. Arrowheads, monomer and multimer of TMEM16F. **c**, 293T cells expressing TMEM16F–mRFP were observed under a fluorescent microscope. Scale bars, 10 μm. **d**, Vector-transformed Ba/F3 cells, or cells expressing wild-type or mutant TMEM16F, were stained with Annexin V with or without pretreatment with BAPTA-AM. **e**, Vector-transformed or wild-type TMEM16F-Ba/F3 cells were preincubated with Annexin V. After addition of A23187, the fluorescence was monitored. The *y* axis shows fluorescence intensity on FACS. **f**, Vector-transformed or mutant TMEM16F-expressing Ba/F3 cells were incubated for 8 min at room temperature (26–27 °C) with 0.5 μM NBD-PtdCho in Hanks balanced salt solution containing Ca^{2+}. After dilution with fatty-acid-free BSA buffer, the fluorescence intensity was determined by FACS. **g**, Vector-transformed or wild-type TMEM16F-expressing Ba/F3 cells were preincubated at 4 °C with 0.1 μM NBD-PtdCho. A23187 (A23) was added and incubated for 8 min at room temperature, and internalized NBD-PtdCho was determined as above. In **f** and **g** the percentage of BSA-non-extractable NBD-PtdCho was determined in triplicate at 4 min (**f**) or 6 min (**g**) after the addition of NBD-PtdCho and is plotted as mean and s.d. All experiments were performed at least three times.

1–12, was identical in the patient and the parents, whereas its 3′ half, corresponding to exons 11–20, was shorter in the patient than in the parents (Fig. 4b). A sequence analysis indicated that the cDNA of the patient lacked the 226-bp sequence corresponding to exon 13. Direct sequencing of the chromosomal DNA indicated that the *TMEM16F* gene of the patient carried a G-to-T homozygous mutation at the splice-acceptor site in intron 12, whereas both parents were heterozygous for the mutation at this position (Fig. 4c). PCR analysis of the *TMEM16F* mRNA with primers at exons 12 and 16 showed a 608-bp band from the control and a 382-bp band from the cell line from the patient with Scott syndrome (Fig. 4d), indicating that a mutation in the splice acceptor site caused exon 13 to be skipped. This skipping caused a frame shift resulting in the premature termination of the protein in exon 14 (Fig. 4e) at the third transmembrane segment of human TMEM16F (Fig. 4f). The nonsense-mediated mRNA decay[21] may explain the decreased concentration of the exon-13-deleted form of *TMEM16F* mRNA in the patient's parents (Fig. 4d).

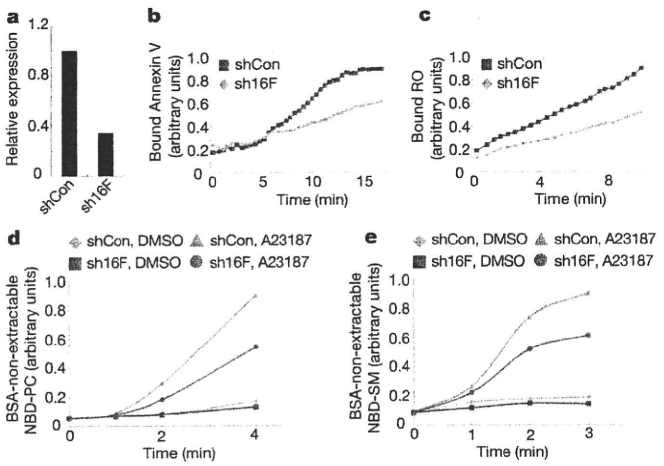

Figure 3 | Requirement of TMEM16F for phospholipid scrambling. **a**, Ba/F3 transformants expressing shRNA for *Tmem16f* (sh16F) or scrambled shRNA (shCon). *Tmem16f* mRNA level was normalized to *β-actin* mRNA and is shown as relative expression. **b**, **c**, Ba/F3 cells expressing sh16F or shCon were preincubated with Cy5-Annexin V (**b**) or biotin-Ro09-0198 (RO) and allophycocyanin (APC)-labelled streptavidin (**c**). A23187 was added and fluorescence was monitored. **d**, **e**, Ba/F3 cells expressing sh16F or shCon were preincubated with 0.5 μM NBD-PtdCho (**d**) or NBD-SM (**e**) in Hanks balanced salt solution containing Ca^{2+}. A23187 was added, incubated and diluted with fatty-acid-free BSA buffer, and fluorescence was determined. Experiments in **b**–**e** were performed at least three times.

Repeated FACS analysis has been used previously to establish cell lines that overexpress a particular cell-surface protein[22,23]. Here, this method yielded TMEM16F carrying a point mutation that rendered the process extremely sensitive to Ca^{2+}, such that in the cells expressing the mutated TMEM16F the phospholipid scramblase functioned even in resting cells, in which the cytosolic Ca^{2+} concentration was below 100 nM (ref. 24). The TMEM16 family, to which TMEM16F belongs, consists of ten members in humans and mice[5]. The founding member of the family, human TMEM16A, is a Ca^{2+}-dependent Cl^- channel[11–13]. Although the direct binding of Ca^{2+} to TMEM16 members has yet to be demonstrated, the amino-terminal region of TMEM16A seems to have a regulatory role[25]. Similarly, the increased sensitivity of the D409G mutant to Ca^{2+} suggests that either Ca^{2+} or a Ca^{2+}-sensing molecule binds to this N-terminal region of TMEM16F. The overexpression of TMEM16A in Ba/F3 cells had no effect on the ionophore-induced exposure of PtdSer (data not shown), suggesting that different members of this family have distinct functions. The PtdSer exposure or scrambling of phospholipids occurs in other biological processes[1,4,26–29], such as apoptotic cell death, the fusion of muscle, bone or trophoblast cells, and the release of neurotransmitters and microvesicles. It will be

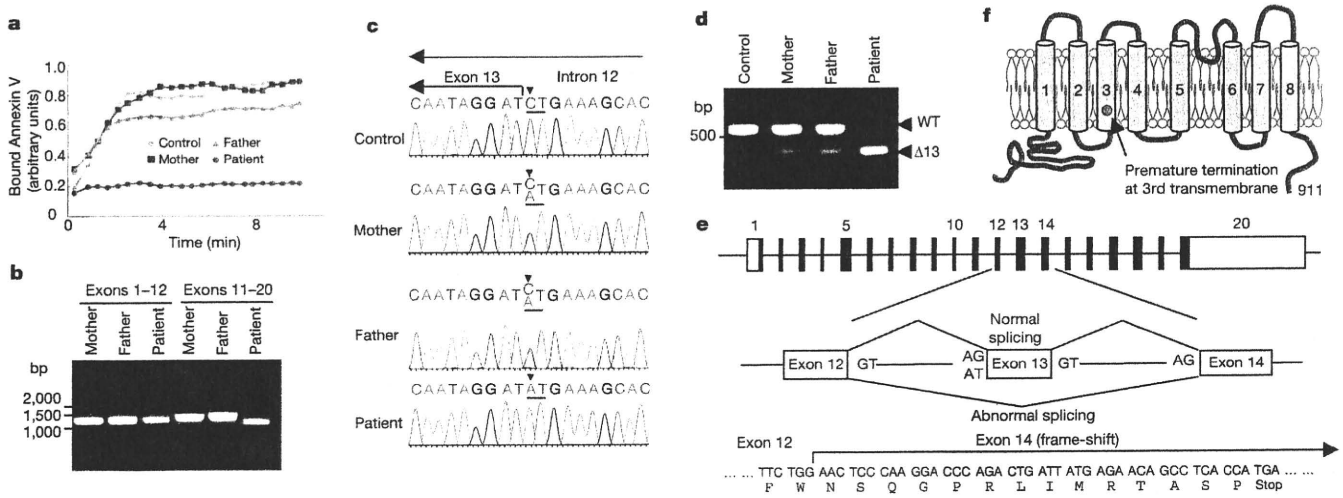

Figure 4 | A splice mutation of *TMEM16F* in a patient with Scott syndrome. **a**, Cells from control, from a patient with Scott syndrome and from the patient's parents, were preincubated with Annexin V. A23187 was added and fluorescence was monitored. **b**, RT–PCR for *TMEM16F* mRNA for exons 1–12 and 11–20 with RNA from the patient and parents. **c**, The junction between exon 13 and intron 12 of the *TMEM16F* gene sequenced from the 3′ end. The CT complementary to the splice acceptor site AG is underlined. Arrowheads indicate the mutation. **d**, RT–PCR for exons 12–16. Arrowheads indicate fragments for the wild-type (WT) and exon-13-deleted forms. **e**, Splicing in the patient's *TMEM16F* gene. The mutation causes the skipping of exon 13, resulting in a frame-shift mutation in exon 14. **f**, Schematic representation of the frame-shift mutation in the Scott patient that causes premature termination in the third transmembrane region of TMEM16F.

interesting to study whether TMEM16F and/or its related members in the TMEM16 family are involved in these processes.

METHODS SUMMARY

To expose PtdSer reversibly on the cell surface, Ba/F3 cells were treated at 37 °C with A23187 under Ca^{2+}-free conditions. The exposed PtdSer was detected by binding of Annexin V at 4 °C in Ca^{2+}-containing Annexin V-binding buffer. A subline (Ba/F3-PS19) of Ba/F3 cells that was extremely sensitive to Ca^{2+}-ionophore-elicited PtdSer exposure was selected by repeating the sorting 19 times with FACSAria (BD Bioscience). A cDNA library was established with mRNA from Ba/F3-PS19 cells in retrovirus vector, and the cDNA (*Tmem16f*) that caused Ba/F3 cells to expose PtdSer constitutively was identified by expression cloning. The Epstein–Barr virus (EBV)-transformed cell lines from a patient with Scott syndrome and from the patient's parents were described previously[20]. The *TMEM16F* mRNA in these cell lines was analysed by RT–PCR. The *TMEM16F* chromosomal gene was amplified by PCR from the genomic DNA of the cell lines, and was directly sequenced by cycle sequencing with an ABI 3100 genetic analyser (Applied Biosystems). Exposure of PtdSer and PtdEtn on the cell surface was analysed by the binding of Cy5-labelled Annexin V and biotin-labelled Ro09-0198 (ref. 17), respectively. The internalization of NBD-PtdCho and NBD-SM was analysed by the BSA-extraction method essentially as described[30]. For the knock-down experiment, shRNA-retrovirus vectors for *Tmem16f* and control scrambled sequence were obtained from OriGene, and the resultant retrovirus was used to infect Ba/F3 cells.

Full Methods and any associated references are available in the online version of the paper at www.nature.com/nature.

Received 19 April; accepted 13 October 2010.
Published online 24 November 2010.

1. Leventis, P. A. & Grinstein, S. The distribution and function of phosphatidylserine in cellular membranes. *Annu. Rev. Biophys.* **39,** 407–427 (2010).
2. Zwaal, R. F., Comfurius, P. & Bevers, E. M. Lipid–protein interactions in blood coagulation. *Biochim. Biophys. Acta* **1376,** 433–453 (1998).
3. Lentz, B. Exposure of platelet membrane phosphatidylserine regulates blood coagulation. *Prog. Lipid Res.* **42,** 423–438 (2003).
4. Balasubramanian, K. & Schroit, A. Aminophospholipid asymmetry: a matter of life and death. *Annu. Rev. Physiol.* **65,** 701–734 (2003).
5. Galietta, L. The TMEM16 protein family: a new class of chloride channels? *Biophys. J.* **97,** 3047–3053 (2009).
6. Weiss, H. & Lages, B. Family studies in Scott syndrome. *Blood* **90,** 475–476 (1997).
7. Zwaal, R., Comfurius, P. & Bevers, E. Scott syndrome, a bleeding disorder caused by defective scrambling of membrane phospholipids. *Biochim. Biophys. Acta* **1636,** 119–128 (2004).
8. Williamson, P. *et al.* Phospholipid scramblase activation pathways in lymphocytes. *Biochemistry* **40,** 8065–8072 (2001).
9. Wielders, S. J. *et al.* Absence of platelet-dependent fibrin formation in a patient with Scott syndrome. *Thromb. Haemost.* **102,** 76–82 (2009).
10. Daleke, D. Phospholipid flippases. *J. Biol. Chem.* **282,** 821–825 (2007).
11. Caputo, A. *et al.* TMEM16A, a membrane protein associated with calcium-dependent chloride channel activity. *Science* **322,** 590–594 (2008).
12. Schroeder, B., Cheng, T., Jan, Y. & Jan, L. Expression cloning of TMEM16A as a calcium-activated chloride channel subunit. *Cell* **134,** 1019–1029 (2008).
13. Yang, Y. *et al.* TMEM16A confers receptor-activated calcium-dependent chloride conductance. *Nature* **455,** 1210–1215 (2008).
14. Schreiber, R. *et al.* Expression and function of epithelial anoctamins. *J. Biol. Chem.* **285,** 7838–7845 (2010).
15. Shi, J. & Gilbert, G. Lactadherin inhibits enzyme complexes of blood coagulation by competing for phospholipid-binding sites. *Blood* **101,** 2628–2636 (2003).
16. Hanayama, R., Tanaka, M., Miwa, K. & Nagata, S. Expression of developmental endothelial locus-1 in a subset of macrophages for engulfment of apoptotic cells. *J. Immunol.* **172,** 3876–3882 (2004).
17. Emoto, K., Toyama-Sorimachi, N., Karasuyama, H., Inoue, K. & Umeda, M. Exposure of phosphatidylethanolamine on the surface of apoptotic cells. *Exp. Cell Res.* **232,** 430–434 (1997).
18. Macia, E. *et al.* Dynasore, a cell-permeable inhibitor of dynamin. *Dev. Cell* **10,** 839–850 (2006).
19. Toti, F., Satta, N., Fressinaud, E., Meyer, D. & Freyssinet, J. Scott syndrome, characterized by impaired transmembrane migration of procoagulant phosphatidylserine and hemorrhagic complications, is an inherited disorder. *Blood* **87,** 1409–1415 (1996).
20. Kojima, H. *et al.* Production and characterization of transformed B-lymphocytes expressing the membrane defect of Scott syndrome. *J. Clin. Invest.* **94,** 2237–2244 (1994).
21. Shyu, A., Wilkinson, M. & van Hoof, A. Messenger RNA regulation: to translate or to degrade. *EMBO J.* **27,** 471–481 (2008).
22. Kavathas, P. & Herzenberg, L. A. Amplification of a gene coding for human T-cell differentiation antigen. *Nature* **306,** 385–387 (1983).
23. Suda, T., Takahashi, T., Golstein, P. & Nagata, S. Molecular cloning and expression of the Fas ligand: a novel member of the tumor necrosis factor family. *Cell* **75,** 1169–1178 (1993).
24. Berridge, M., Bootman, M. & Roderick, H. Calcium signalling: dynamics, homeostasis and remodelling. *Nature Rev. Mol. Cell. Biol.* **4,** 517–529 (2003).
25. Ferrera, L. *et al.* Regulation of TMEM16A chloride channel properties by alternative splicing. *J. Biol. Chem.* **284,** 33360–33368 (2009).
26. Nagata, S., Hanayama, R. & Kawane, K. Autoimmunity and the clearance of dead cells. *Cell* **140,** 619–630 (2010).
27. Huppertz, B., Bartz, C. & Kokozidou, M. Trophoblast fusion: fusogenic proteins, syncytins and ADAMs, and other prerequisites for syncytial fusion. *Micron* **37,** 509–517 (2006).
28. Helming, L. & Gordon, S. Molecular mediators of macrophage fusion. *Trends Cell Biol.* **19,** 514–522 (2009).
29. van den Eijnde, S. *et al.* Transient expression of phosphatidylserine at cell–cell contact areas is required for myotube formation. *J. Cell Sci.* **114,** 3631–3642 (2001).
30. Williamson, P. *et al.* Transbilayer phospholipid movements in ABCA1-deficient cells. *PLoS ONE* **2,** e729 (2007).

Supplementary Information is linked to the online version of the paper at www.nature.com/nature.

Acknowledgements We thank T. Wiedmer for critical reading of our manuscript, and M. Fujii and M. Harayama for secretarial assistance. This work was supported in part by Grants-in-Aid for Specially Promoted Research (to S.N.) and for Young Scientists Start-up (to J.S.) from the Japan Society for the Promotion of Science. J.S. is supported by a research fellowship from the Japan Society for the Promotion of Science. P.J.S. was supported by grants from the National Institutes of Health, USA.

Author Contributions J.S. designed and performed the experiments, and wrote the manuscript. M.U. provided biotin-labelled Ro09-0198 peptide. P.J.S. provided EBV-transformed cell lines from a patient and the patient's parents, and commented on the manuscript. S.N. was responsible for the overall study design and for writing the manuscript.

Author Information Reprints and permissions information is available at www.nature.com/reprints. The authors declare no competing financial interests. Readers are welcome to comment on the online version of this article at www.nature.com/nature. Correspondence and requests for materials should be addressed to S.N. (snagata@mfour.med.kyoto-u.ac.jp).

METHODS

Cell lines, recombinant proteins, antibodies, serum and reagents. Mouse interleukin (IL-3)-dependent Ba/F3 cells were maintained in RPMI medium containing 10% fetal calf serum (FCS; Gibco), 45 U ml^{-1} recombinant mouse IL-3 and 50 μM 2-mercaptoethanol. The EBV-transformed human cell lines[20] from a patient with Scott syndrome and the patient's parents were grown in RPMI1640 medium containing 10% FCS and 50 μM 2-mercaptoethanol. Human 293T cells and Plat-E packaging cells[31] were cultured in DMEM medium containing 10% FCS. Recombinant mouse IL-3 was produced by mouse C127I cells transformed with a bovine papillomavirus expression vector bearing mouse *Il-3* cDNA as described[32]. Biotin-labelled Ro09-0198 was prepared as described previously[33]. Flag-tagged mouse MFG-E8 was produced in human 293T cells as described[34], and the secreted MFG-E8 was purified with anti-Flag M2 beads (Sigma-Aldrich).

Ca^{2+}/Mg^{2+}-free RPMI1640 medium was purchased from Cell Science & Technology Institute. Ca^{2+}-free RPMI medium contained 0.5 mM $MgSO_4$. Ca^{2+}-free FCS was prepared by dialysing FCS for 2 days against PBS, with four changes of buffer. Dynasore was purchased from Calbiochem.

BAPTA-AM was from Dojindo. NBD-PtdCho and NBD-SM were purchased from Avanti Polar Lipids.

Treatment with Ca^{2+} ionophore, flow cytometry, and cell sorting. To expose PtdSer on the cell surface, 2×10^5 cells in a 96-well microtitre plate were washed with PBS, resuspended in 200 μl of HBSS (Gibco) and treated with A23187 (Sigma-Aldrich) at 37 °C for 15 min. The cells were stained on ice for 15 min with 2,500–5,000-fold diluted Cy5-labelled Annexin V (Biovision) in staining buffer (10 mM Hepes-NaOH pH 7.4 containing 140 mM NaCl and 2.5 mM $CaCl_2$) in the presence of 5 μg ml^{-1} PI. Flow cytometry was performed on a FACSAria (BD Bioscience) or FACSCalibur (BD Bioscience) and the data were analysed with FlowJo Software (True Star).

A subline of Ba/F3 cells that was sensitive to Ca^{2+}-ionophore-elicited PtdSer exposure was selected by repetitive sorting with a FACSAria. In brief, after 2×10^7 Ba/F3 cells in HBSS had been treated at 37 °C for 15 min with A23187, they were suspended in 1 ml of Annexin V staining buffer that had been prechilled to 4 °C. The cells were stained with Cy5-Annexin V on ice as described above, and sorted with a FACSAria whose injection chamber was kept at 4 °C. Cells providing the highest level of Cy5 fluorescence signal (the top 0.5–5.0%) were collected and resuspended at a density of more than 10^5 cells ml^{-1} in Ca^{2+}-free RPMI containing 5% dialysed FCS, 45 U ml^{-1} IL-3 and 50 μM 2-mercaptoethanol. After 24 h the cells were resuspended in normal Ca^{2+}-containing RPMI medium and expanded for the next sorting.

Construction of the cDNA library. Total RNA was prepared from Ba/F3 PS19 cells with an RNeasy Mini Kit (Qiagen), and poly(A)$^+$ RNA was purified with an mRNA Purification Kit (GE Healthcare) with two cycles of oligo(dT)-cellulose column chromatography. Double-stranded cDNA was synthesized with random hexamers as primers, using a cDNA synthesis kit (SuperScript Choice System for cDNA Synthesis; Invitrogen). A *Bst*XI adaptor was attached, and the fragments were size-fractionated by electrophoresis through a 1% agarose gel (Seakem GTG agarose; Lonza). DNA fragments longer than 2.5 kb were recovered from the gel with a DNA extraction kit (Wizard SV Gel and PCR Clean-up System; Promega) and ligated into a *Bst*XI-digested pMXs vector[35]. *Escherichia coli* DH10B cells (ElectroMax DH10B; Invitrogen) were transformed by electroporation with a Gene Pulser (Bio-Rad). About 9.3×10^5 clones were produced, and plasmid DNA was prepared with a QIAfilter Plasmid Maxi Kit (Qiagen).

Cell fusion. Ba/F3-PS0 and Ba/F3-PS19 cells were transduced with pMXs-puro EGFP and pMXs-neo DsRed, respectively, and cultured in the presence of 1 μg ml^{-1} puromycin or 1 mg ml^{-1} G418. Ba/F3-PS0 EGFP cells and Ba/F3-PS19 DsRed cells were fused in the presence of PEG1500 and cultured in the presence of 1 μg ml^{-1} puromycin and 1 mg ml^{-1} G418. The EGFP/DsRed double-positive cells were sorted with a FACSAria.

Screening of cDNA library. Plasmid DNA (108 μg) from the cDNA library was introduced by lipofection with FuGENE6 (Roche Diagnostics) into 7.2×10^7 PLAT-E packaging cells[31] grown in eighteen 10-cm dishes. Two days after the transfection, the viruses in the culture supernatant were centrifuged at 4 °C and 6,000*g* for 16 h, resuspended in RPMI1640 medium containing 10% FCS and 45 U ml^{-1} IL-3, and used to infect 7.2×10^6 Ba/F3 cells in the presence of 8 μg ml^{-1} Polybrene (Sigma-Aldrich). After a 24-h culture, the medium was replaced with fresh medium, and the cells were further cultured for 2 days. The sorting of cells that were sensitive to ionophore-induced PtdSer exposure was performed as described above.

Isolation of cDNA fragments from Annexin V-positive Ba/F3 cells. To isolate the cDNA integrated into the retroviral vector, the genomic DNA was extracted from Ba/F3 cell transformants with the Wizard Genomic DNA Purification System (Promega) and subjected to PCR with the Expand Long Template PCR System (Roche Diagnostics). The PCR primers (5′-CCCGGGGGTGGACCATCCTCT-3′ and 5′-CCCCTTTTTCTGGAGACTAAAT-3′) carried sequences from the pMXs vector, and the conditions for PCR were 10 s at 96 °C, 30 s at 58 °C and 4 min at 68 °C for 35 cycles. The PCR fragments were cloned into the pGEM-T Easy vector (Promega) and subjected to DNA sequencing analysis with an ABI PRISM 3100 Genetic Analyser (Applied Biosystems).

Expression vector for TMEM16F and its mutants. The Flag-tag sequence was integrated into the *Eco*RI and *Xho*I sites of the retroviral vector pMXs-puro, resulting in pMXs-puro c-Flag. The full-length coding sequence for mouse TMEM16F (GenBank accession number NM_175344) was prepared by RT–PCR with the mRNA from Ba/F3 cells. The primers used were as follows (in each primer the *Eco*RI recognition sequence is underlined): 5′-ATATGAATTCGACATGCAGATG ATGACTAGGAA-3′ and 5′-ATATGAATTCGAGTTTTGGCCGCACGCTGT-3′.

The PCR fragments were inserted into the *Eco*RI site of pMXs-puro c-Flag, and the authenticity of the cDNAs was verified by DNA sequencing.

For the expression plasmid of TMEM16F–mRFP, the coding sequence for mRFP in pcDNA-mRFP (Invitrogen) was joined in-frame to the C terminus of mouse TMEM16F and introduced into pMXs vector.

Expression in mouse Ba/F3 and human 293T cells. The expression vector for Flag-tagged TMEM16F in pMXs-puro was introduced into Plat-E cells. The retrovirus produced was concentrated as described above and used to infect Ba/F3 cells to establish stable transformants. The transformants were selected by culturing the cells in medium containing puromycin (1.0 μg ml^{-1}). To express TMEM16F–mRFP, human 293T cells were transfected by lipofection with FuGENE6 with the pMXs vector carrying the TMEM16F–mRFP sequence. One day later, the transfected cells were observed by fluorescence microscopy (BioRevo BZ-9000; Keyence).

Western blotting. Cells were lysed in RIPA buffer (50 mM Hepes-NaOH pH 8.0 containing 1% Nonidet P40, 0.1% SDS, 0.5% sodium deoxycholate, 150 mM NaCl and 10% protease inhibitor cocktail (Complete Mini; Roche Diagnostics)). The lysate was mixed with 5 × SDS sample buffer (200 mM Tris-HCl pH 6.8, 10% SDS, 25% glycerol, 5% 2-mercaptoethanol, 0.05% bromophenol blue), boiled for 5 min and separated by electrophoresis on a 10% polyacrylamide gel (Bio Craft). After the proteins had been transferred to a poly(vinylidene difluoride) membrane (Millipore), the membranes were probed with horseradish peroxidase-conjugated mouse anti-Flag M2 (Sigma), and peroxidase activity was detected with a Western Lightning enhanced chemiluminescence system (PerkinElmer).

RT–PCR of *TMEM16F* cDNA and sequencing of its chromosomal gene in a patient with Scott syndrome. Total RNA was prepared from EBV-transformed cell lines from a patient with Scott syndrome and from the patient's parents, and from a healthy control. The RNA was reverse-transcribed with Superscript III (Invitrogen), in accordance with the manufacture's protocol, and the *TMEM16F* cDNA was analysed by PCR with the following sets of primers (in each primer the additional sequence is underlined): Ex1-FW (5′-ATATGAATTCGACATGA AAAAGATGAGCAGGAA-3′), Ex11/12-RV (5′-GCGTTCTTCTTCCTGAGT AA-3′), Ex11/12-FW (5′-TTACTCAGGAAGAAGAACGC -3′), Ex20-RV (5′-ATATGAATTCTTCTGATTTTGGCCGTAAAT-3′), Ex12-FW (5′- TCTGTG CCAGTGCTGTCTTT-3′) and Ex16-RV (5′- CTGCAGATGGTAGTCCTGTT-3′).

For the sequence analysis of the human *TMEM16F* chromosomal gene, genomic DNA was prepared from human cell lines and a 965-bp DNA fragment carrying the 226-bp exon 13 and its 5′-flanking and 3′-flanking regions (about 370 bp each) was amplified by PCR with the following primers: 5′-CCA GAGTATGCTACTAGTTG-3′ and 5′-TCTCAGCAACCGAGGAACAT-3′. The PCR products were purified with a Wizard SV PCR and Gel Clean-up System. Cycle sequencing was performed with a BigDye Terminator v3.1 Cycle Sequencing kit with a primer of 5′-GGACCTTACCGAAGTTAGTA-3′, and analysed with an ABI PRIZM 3100 Genetic Analyser.

Analysis of exposure of PtdSer and PtdEtn. To analyse the exposure of PtdSer and PtdEtn, 10^5 cells at early exponential phase were washed with PBS, suspended in 1.0 ml of cold Annexin V staining buffer with 2,500–5,000-fold diluted Cy5-labelled Annexin V or 800-fold diluted biotin-Ro09-0198 (ref. 33) followed by 1.0 μg ml^{-1} APC-labelled streptavidin and 5 μg ml^{-1} PI. The samples were incubated on ice for 15 min, and flow cytometry was performed on a FACSAria or FACSCalibur as described above. For binding of MFG-E8, the cells were suspended in RPMI1640 containing 10% FCS and then incubated on ice for 20 min with Flag-tagged D89E mutant of MFG-E8 (0.4 μg ml^{-1})[34]. The cells were washed with the above medium and incubated on ice for 20 min with 1.0 μg ml^{-1} hamster monoclonal antibody against mouse MFG-E8 (clone 2422). This was followed by incubation with phycoerythrin-labelled mouse anti-hamster IgG (BD Bioscience) and analysis by flow cytometry with a FACSAria.

To study the requirement for intracellular Ca^{2+}, 10^5 cells were incubated with 10 μM BAPTA-AM in RPMI1640 medium containing 10% FCS at 37 °C for 5 min for the PtdSer exposure, or for 60 min for the PtdEtn exposure. The cells were

washed with Annexin V staining buffer, and stained with Cy5-Annexin V or biotin-Ro09-0198 as described above.

For the kinetic study of the Ca^{2+}-induced PtdSer and PtdEtn exposure, 10^6 cells were washed with PBS, suspended in 1.0 ml of cold Annexin V staining buffer with Cy5-labelled Annexin V or a mixture of biotin-Ro09-0198 and APC-labelled streptavidin, and 5 $\mu g\,ml^{-1}$ PI. Cells were mixed on ice with A23187 at a final concentration of 0.25 or 0.5 μM, and applied to the injection chamber of a FACSAria that was set at 20 °C (for Ba/F3 cells) or 37 °C (for human cell lines) to induce the A23187 reaction. Data were recorded for the indicated periods, and the PI-positive cells were excluded from the analysis.

Internalization of NBD-PtdCho and NBD-SM. The internalization of NBD-lipid analogues was analysed by flow cytometry essentially as described in refs 8 and 30. In brief, 10^6 cells were washed with HBSS and resuspended in 0.5 ml of HBSS containing 2 mM $CaCl_2$ (HBSS-Ca). An equal volume of HBSS-Ca containing 1 μM NBD-PtdCho or NBD-SM was added to the cell suspension and incubated at room temperature. At each time point, 150 μl of cell suspension was collected, mixed with 150 μl of the prechilled (4 °C) HBSS-Ca containing 5 mg ml^{-1} fatty-acid-free BSA (Sigma-Aldrich), to extract the unincorporated fluorescent lipids, and 500 nM Sytoxblue (Molecular Probes). To measure the total fluorescence, samples were mixed with HBSS-Ca in the absence of BSA. After incubation for 10 min at 4 °C to extract the lipid, the cells were analysed with a FACSAria for forward scatter, side scatter, logarithmic green fluorescence (NBD), and Sytoxblue fluorescence. The Sytoxblue-positive dead cells were excluded from the analysis. The fluorescence of NBD-phospholipids that were resistant to the BSA extraction was regarded as representing phospholipids that had been incorporated into cells.

To examine the effect of the Ca^{2+} ionophore, 5×10^5 cells were washed with HBSS-Ca, resuspended in 0.5 ml of cold HBSS-Ca, and incubated on ice for 7 min. Cold HBSS (0.5 ml) containing 0.2 μM NBD-PtdCho or NBD-SM was added to the cell suspension and incubated further on ice for 3 min. The cells were then mixed with A23187 and incubated at room temperature to induce lipid incorporation. A 150-μl aliquot was used to determine the incorporated lipid quantity as described above.

Thin-layer chromatography. After incubation of cells with NBD-PtdCho or NBD-SM, the phospholipids were extracted from the cells by incubation at room temperature for 30 min with a mixture of chloroform, methanol and water (5:10:4, by volume). The phospholipids were separated by thin-layer chromatography on a silica gel 60 plate (Merck) with chloroform/acetone/methanol/acetic acid/water (5:2:1:1:0.5 by volume) as a solvent. The fluorescence on the plate was detected with a LAS4000 image analyser (Fuji Film).

Intracellular Ca^{2+} and Ca^{2+} influx. To determine the intracellular Ca^{2+} concentration, 10^6 cells were suspended in HBSS, incubated at 37 °C for 10 min with 0.4 μM Fluo-4-AM (Molecular Probes), washed with HBSS, and analysed with a FACSAria.

The Ca^{2+} influx was measured as described[36]. In brief, 10^6 cells were labelled for 30 min at 37 °C with 1 μM Fluo-4-AM in RPMI containing 10% FCS. After being washed with the Annexin V staining buffer, the cells were kept at 4 °C in Annexin V staining buffer. The Ca^{2+} ionophore A23187 was added to the mixture at a final concentration of 0.5 μM, and the change in mean fluorescence intensity was directly recorded with a FACSCalibur system. The data was analysed with FlowJo Software.

shRNA. shRNA expression plasmids for mouse *Tmem16f* in a pRS shRNA vector carrying the puromycin-resistance gene were purchased from OriGene. The target sequence of the shRNA for *Tmem16f* was 5′-CATCTACTCTGTGAAGTTC TTCATTTCCT-3′. The scrambled non-effective shRNA (5′-GCACTACCAGA GCTAACTCAGATAGTACT-3′) in pRS was from OriGene. Ba/F3 cells were infected with retrovirus containing the shRNA, and cultured in the presence of 1.0 $\mu g\,ml^{-1}$ puromycin. Puromycin-resistant cells were subjected to cloning by limited dilution. The *Tmem16f* mRNA was quantified by real-time PCR, and the clones that showed the decreased expression were used for further study.

31. Morita, S., Kojima, T. & Kitamura, T. Plat-E: an efficient and stable system for transient packaging of retroviruses. *Gene Ther.* **7,** 1063–1066 (2000).
32. Fukunaga, R., Ishizaka-Ikeda, E. & Nagata, S. Purification and characterization of the receptor for murine granulocyte colony-stimulating factor. *J. Biol. Chem.* **265,** 14008–14015 (1990).
33. Aoki, Y., Uenaka, T., Aoki, J., Umeda, M. & Inoue, K. A novel peptide probe for studying the transbilayer movement of phosphatidylethanolamine. *J. Biochem.* **116,** 291–297 (1994).
34. Hanayama, R. *et al.* Identification of a factor that links apoptotic cells to phagocytes. *Nature* **417,** 182–187 (2002).
35. Kitamura, T. *et al.* Retrovirus-mediated gene transfer and expression cloning: powerful tools in functional genomics. *Exp. Hematol.* **31,** 1007–1014 (2003).
36. Bernhagen, J. *et al.* MIF is a noncognate ligand of CXC chemokine receptors in inflammatory and atherogenic cell recruitment. *Nature Med.* **13,** 587–596 (2007).

Cytokine-dependent but acquired immunity-independent arthritis caused by DNA escaped from degradation

Kohki Kawane[a,1], Hiromi Tanaka[a], Yusuke Kitahara[a,b], Shin Shimaoka[c], and Shigekazu Nagata[a,d,2]

[a]Department of Medical Chemistry, Kyoto University Graduate School of Medicine, Kyoto 606-8501, Japan; [b]Osaka University Medical School, Osaka 565-0871, Japan; [c]Fuji Gotemba Research Laboratories, Chugai Pharmaceutical Co., Shizuoka 412-8513, Japan; and [d]Core Research for Evolutional Science and Technology, Japan Science and Technology Corporation, Kyoto 606-8501, Japan

Edited by Ruslan Medzhitov, Yale University School of Medicine, New Haven, CT, and approved September 29, 2010 (received for review July 20, 2010)

DNase II digests the chromosomal DNA in macrophages after apoptotic cells and nuclei from erythroid precursors are engulfed. The DNase II-null mice develop a polyarthritis that resembles rheumatoid arthritis. Here, we showed that when bone marrow cells from the DNase II-deficient mice were transferred to the wild-type mice, they developed arthritis. A deficiency of Rag2 or a lack of lymphocytes accelerated arthritis of the DNase II-null mice, suggesting that the DNase II$^{-/-}$ macrophages were responsible for triggering arthritis, and their lymphocytes worked protectively. A high level of TNFα, IL-1β, and IL-6 was found in the affected joints of the DNase II-null mice, suggesting an inflammatory-skewed cytokine storm was established in the joints. A lack of TNFα, IL-1β, or IL-6 gene blocked the expression of the other cytokine genes as well and inhibited the development of arthritis. Neutralization of TNFα, IL-1β, or IL-6 had a therapeutic effect on the developed arthritis of the DNase II-null mice, indicating that the cytokine storm was essential for the maintenance of arthritis in the DNase II-deficient mice. Methotrexate, an antimetabolite that is often used to treat patients with rheumatoid arthritis, had a therapeutic effect with the DNase II-null mice. These properties of arthritis in the DNase II-null mice were similar to those found in human systemic-onset juvenile idiopathic arthritis or Still's disease, indicating that the DNase II-null mice are a good animal model of this type of arthritis.

inflammation | macrophages | apoptosis | DNase II | engulfment

Rheumatoid arthritis (RA), defined as a proliferative inflammation of the synovial membranes in multiple joints, is a chronic disease that afflicts up to 0.5–1% of the population (1). RA has been considered an autoimmune disease that involves T cells (2), B cells, or autoantibodies (3), macrophages (4), and inflammatory cytokines, such as TNFα, IL-1β, and IL-6 (5). However, the etiology of RA remains elusive, particularly owing to its complex heterogeneity.

Each mammalian cell carries about 6 pg of DNA, which is actively degraded by a group of enzymes (DNases) in physiological situations (6, 7). DNase II located in lysosomes (8) digests the DNA of apoptotic cells and of nuclei expelled from erythroid precursors (9, 10). DNase II$^{-/-}$ mice accumulate undigested DNA in the lysosomes of macrophages, which activates the macrophages to produce IFNβ. The elevated level of IFNβ causes lethal anemia in mouse embryos (11). DNase II$^{-/-}$ mice that also lack the type I IFN receptor (IFN-IR$^{-/-}$) can live to adulthood, but develop chronic polyarthritis resembling RA (12). When the DNase II gene is inducibly deleted in adult mice, using the Mx1-Cre/loxP system, the mice (DNase II$^{\Delta/-}$) also develop polyarthritis.

In both types of DNase II-null mice (DNase II$^{-/-}$IFN-IR$^{-/-}$ and DNase II$^{\Delta/-}$), the joints start to swell visibly around 2 mo of age, and the swelling gets worse over time. At this stage, the digits are deformed and difficult to bend at the joints. Histologically, cartilage destruction and bone erosion are evident in the affected joints. Proliferated synoviocytes, macrophages, and fibroblasts make up the pannus-like structure in the joints, where lymphocytes and neutrophils are also present. Genes for matrix metalloproteinase (MMP)-3 and inflammatory cytokines, including TNFα, IL-1β, and IL-6, are strongly activated in the affected joints.

Here we showed that the lack of the DNase II gene in bone marrow-derived cells is sufficient for the development of arthritis in the DNase II-null mice. The inhibition of TNFα, IL-1β, or IL-6 function blocked the gene expression for all of the inflammatory cytokines (TNFα, IL-1β, and IL-6) in the joints, and prevented arthritis. On the other hand, the lack of lymphocytes resulting from a Rag2-null mutation accelerated the development of arthritis. Methotrexate and anticytokine therapies, which are widely used to treat RA in humans, were also effective in the DNase II-null mice. The pathology of the RA-like arthritis in the DNase II-null mice and its response to cytokine inhibition are similar to systemic-onset juvenile idiopathic arthritis (soJIA). We propose that the activation of macrophages that leads to a cytokine storm in the joints can be one of the etiologies of RA.

Results

Deletion of the DNase II Gene in Bone Marrow-Derived Cells Causes Arthritis. To investigate whether the immune system is activated in the DNaseII-null mice, we analyzed by FACS their splenocytes. At age 1–2.5 mo, around the onset of arthritis, DNase II$^{-/-}$ IFN-IR$^{-/-}$ mice developed splenomegaly, which was mainly caused by the expansion of Ter119^{+} erythroid population (Fig. 1*A*). The number of CD3^{+} T cells and B220^{+} B cells in the DNase II$^{-/-}$IFN-IR$^{-/-}$ mice was comparable to that in control mice, but the populations of activated CD4^{+} and CD8^{+} T cells, estimated by the CD69 expression, were increased from 11 to 27%, and 5 to 23%, respectively, by the DNase II null mutation (Fig. 1*B*). The serum concentration of IgG and anti-double stranded DNA antibodies was elevated in DNase II$^{-/-}$IFN-IR$^{-/-}$ mice (12), and the number of neutrophils, macrophages, and dendritic cells increased by seven-, two-, and threefold, respectively (Fig. 1*A*). To examine the involvement of hematopoietic cells in the arthritis of the DNase II-null mice, 1-mo-old WT mice were exposed to γ-rays, and bone marrow cells from DNase II$^{\Delta/-}$ (poly(I):poly(C)-injected DNaseII$^{flox/-}$Mx1-Cre^{T} mice) or WT mice were transplanted i.v. into the irradiated mice. The mice that received the DNase II-null, but not the WT, bone marrow cells started to develop arthritis 10 wk after the transplantation (Fig. 1*C*), accompanied by an increase in serum MMP-3 (Fig. 1*D*), a marker used to diagnose arthritis (13), indicating that the loss of

Author contributions: K.K., S.S., and S.N. designed research; K.K., H.T., Y.K., and S.S. performed research; K.K., H.T., Y.K., S.S., and S.N. analyzed data; and K.K. and S.N. wrote the paper.

The authors declare no conflict of interest.

This article is a PNAS Direct Submission.

[1]Present address: Institut de Biologie du Développement de Marseille-Luminy, UMR 6216, Case 907, Parc Scientifique de Luminy, 13288 Marseille, Cedex 09, France.

[2]To whom correspondence should be addressed. E-mail: snagata@mfour.med.kyoto-u.ac.jp.

This article contains supporting information online at www.pnas.org/lookup/suppl/doi:10.1073/pnas.1010603107/-/DCSupplemental.

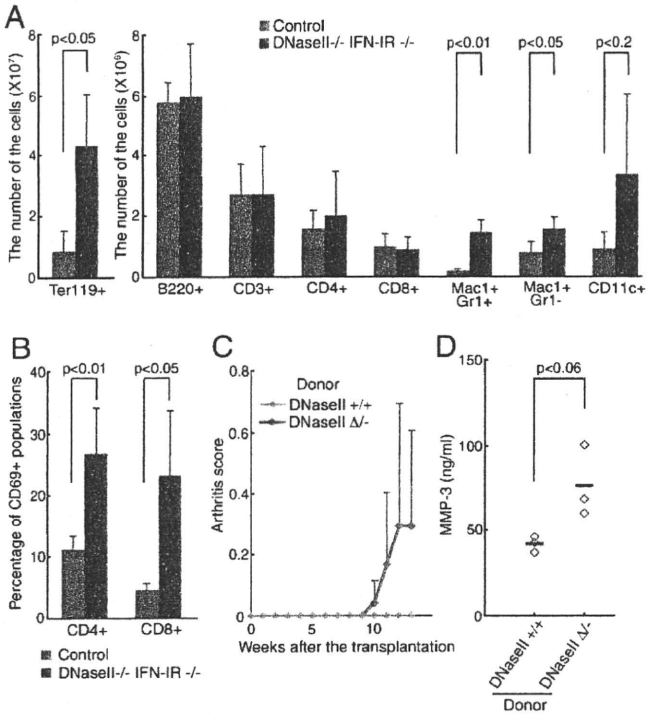

Fig. 1. Activation of lymphocytes in DNase II-null mice and bone marrow transfer. (*A* and *B*) A FACS analysis of splenocytes from 1- to 2.5-mo-old DNase $II^{-/-}$IFN-$IR^{-/-}$ and DNase $II^{+/-}$ or $^{+/+}$IFN-$IR^{-/-}$ littermate mice (control) ($n = 4$ for each group). The average cell number of the indicated cell type (*A*), and the average percentage of $CD69^+$ cells in the $CD4^+$ or $CD8^+$ T cell population (*B*) are shown with SD. (*C* and *D*) Cells from the bone marrow of DNase $II^{\Delta/-}$ or WT mice were transplanted into irradiated 1-mo-old WT mice. Mean arthritis scores at the indicated time after the transplantation were plotted with SD (n = 3–4 for each condition) (*C*). Three months after the transplantation, the serum MMP-3 was quantified by ELISA. The mean values are indicated (bars) (*D*). In *A*, *B*, and *D*, *P* value is shown when it is <0.2.

the DNase II gene in the bone marrow-derived cells was sufficient to cause this arthritis.

No Requirement of Lymphocytes for the Arthritis in DNase II-Null Mice. Lymphocytes are involved in various models of arthritis (2, 3). On the other hand, when a $Rag2^{-/-}$ mutation that blocks the development of lymphocytes was introduced into DNase $II^{-/-}$IFN-$IR^{-/-}$ mice, the DNase $II^{-/-}$IFN-$IR^{-/-}Rag2^{-/-}$ mice developed arthritis with a more accelerated time frame than the DNase $II^{-/-}$IFN-$IR^{-/-}Rag2^{+/+}$ mice (Fig. 2*A*). A histological analysis of the joints of the DNase $II^{-/-}$IFN-$IR^{-/-}Rag2^{-/-}$ mice revealed massive inflammation accompanied by pannus formation, cartilage destruction, and bone erosion (Fig. 2*B*). The MMP-3 gene was up-regulated by more than 40-fold in the joints of the DNase $II^{-/-}$IFN-$IR^{-/-}Rag2^{-/-}$ mice, which was significantly higher than in DNase $II^{-/-}$IFN-$IR^{-/-}Rag2^{+/-}$ mice (Fig. 2*C*). The genes for the inflammatory cytokines TNFα, IL-1β, and IL-6 were expressed in the joints of the DNase $II^{-/-}$IFN-$IR^{-/-}Rag2^{-/-}$ mice, although at a slightly lower level than in those of the Rag2-expressing mice. The genes for the antiinflammatory cytokines TGFβ and IL-10 are expressed in the joints of RA patients as a feedback response to the chronic inflammation (14). These genes were also up-regulated 1.6- and 20.0-fold, respectively, in the DNase $II^{-/-}$IFN-$IR^{-/-}Rag2^{+/-}$ joints compared with the WT joints (Fig. 2*C*). The TGFβ mRNA level was not significantly affected by the Rag2-null mutation, but the IL-10 mRNA level was reduced to 20% of that in the $Rag2^{+/-}$DNase II-null mice. These results suggest that most of the IL-10 in the affected joints of the DNase II-null mice is produced by the lymphocytes recruited to the joints, and that IL-10 inhibits the development of the arthritis, which seems to be consistent with the previous report (15).

IL-17 is produced by Th17 cells, and it seems to contribute to human RA (16). The mRNA encoding IL-17A, a representative cytokine in the IL-17 family, was about 50-fold higher in the inflamed joints of DNase II-null mice than in those of WT mice. The Rag2-mutation significantly reduced the IL17A mRNA level in the joints, but it was still 19 times greater than in control mice, indicating that IL-17 is produced not only by Th17 cells but also by nonlymphoid cells in the joints as reported previously (17).

TNFα-Dependent Arthritis. We previously showed that a neutralizing anti-TNFα mAb inhibits the development of arthritis in DNase II-null mice (12). To confirm the requirement for TNFα, DNase $II^{\Delta/-}$ mice were established on a background of the WT ($TNFα^{+/+}$), heterozygous ($TNFα^{+/-}$), or homozygous ($TNFα^{-/-}$) null mutation of the TNFα gene. As shown in Fig. 3*A*, the DNase $II^{\Delta/-}TNFα^{+/-}$ mice developed arthritis with delayed kinetics, whereas the DNase $II^{\Delta/-}TNFα^{-/-}$ mice did not develop arthritis even 10 mo after poly(I):poly(C) injection. A histological analysis of the DNase $II^{\Delta/-}TNFα^{-/-}$ mice showed that although heavy accumulation of DNA could be found in their bone marrow (Fig. S1*A*), the synovial tissues and joints were intact (Fig. 3*B*). The MMP-3 mRNA level in the joints was also normal (Fig. 3*C*). The deletion of the TNFα gene blocked the up-regulation of the IL-1β and IL-6 mRNA in the joints of the DNase II-null mice. That is, the IL-1β and IL-6 mRNA levels 9–12 mo after the poly(I):poly(C) injection were equivalent to their levels in the poly(I):poly(C)-injected control littermate mice (DNase $II^{flox/+}$Mx1-Cre^T) (Fig. 3*C*). In agreement with the delayed but eventually full-blown development of the arthritis in the DNase $II^{\Delta/-}TNFα^{+/-}$ mice, the IL-1β and IL-6 mRNA levels in their affected joints 9–12 mo after the poly(I):poly(C) injection were similar to those observed in the DNase $II^{\Delta/-}TNFα^{+/+}$ mice. We thus concluded that TNFα plays an essential and rate-limiting role in the arthritis of DNase II-null mice, and its expression in the joints up-regulates the expression of other cytokine genes.

IL-6 and IL-1β, but Not IL-18 Dependence of Arthritis. IL-6 plays an important pathological role in a number of inflammatory diseases (18). To examine its role in arthritis of the DNase II-null mice, the DNase $II^{flox/-}$ Mx1-Cre^T locus was transferred to $IL\text{-}6^{-/-}$ mice, and the mice were treated with poly(I):poly(C). As shown in Fig. S1*A*, the loss of the IL-6 gene had no effect on the accumulation of DNA in the macrophages in the bone marrow. However, the development of arthritis in the DNase$II^{\Delta/-}IL\text{-}6^{+/-}$ mice was delayed, and a null mutation of the IL-6 gene completely blocked the development of arthritis (Fig. 4*A*). No pannus was observed in the joints, and the cartilage and bone were intact (Fig. 4*B*), and the MMP-3 gene was not up-regulated in the joints of the DNase$II^{\Delta/-}IL\text{-}6^{-/-}$ mice (Fig. 4*C*). The lack of IL-6 completely blocked the up-regulation of the TNFα and IL-1β gene expression in the joints of the DNase $II^{\Delta/-}$ mice, indicating that IL-6 transcriptionally regulates the expression of the TNFα and IL-1β genes in the DNase II-null mice.

We next evaluated the contribution of IL-1β to the development of arthritis by treating the mice with an mAb (clone 35F5) against IL-1 receptor (19). Starting when they were 1 mo old, DNase $II^{-/-}$IFN-$IR^{-/-}$ mice were given an i.p. injection every 5 d of rat control IgG or 35F5 mAb. By the age of 3.5 mo, the DNase $II^{-/-}$IFN-$IR^{-/-}$ mice treated with the control IgG showed joint swelling and high serum MMP-3 (Fig. 5 *A* and *B*). In contrast, the joint swelling and high serum MMP-3 level were not observed in the mice that received the 35F5 mAb. The levels of TNFα, IL-1β, and IL-6 mRNA in the joints of the DNase II-null mice were reduced to a negligible level by blocking the IL-1 receptor signal (Fig. 5*C*). Thus, the IL-1 system is also required for the development of arthritis in the DNase II-null mice, and once the IL-1β gene is activated in the joints, it regulates the expression of the TNFα and IL-6 genes.

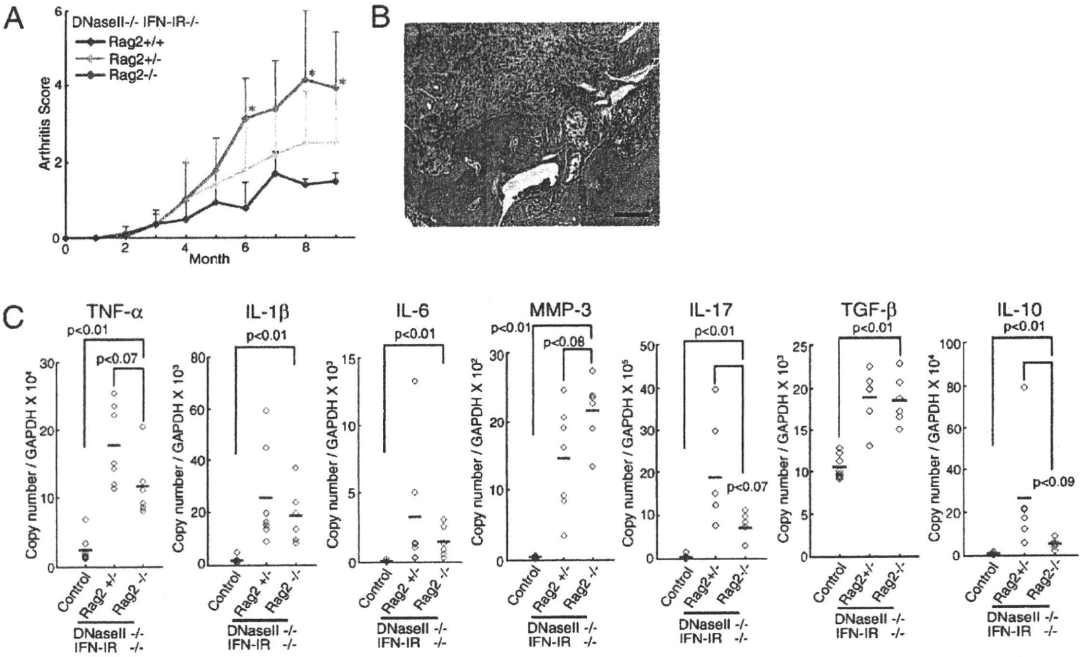

Fig. 2. Development of arthritis in DNase $II^{-/-}IFN\text{-}IR^{-/-}Rag2^{-/-}$ mice. (*A*) Arthritis scores of DNase $II^{-/-}IFN\text{-}IR^{-/-}Rag2^{+/+}$, DNase $II^{-/-}IFN\text{-}IR^{-/-}Rag2^{+/-}$, and DNase $II^{-/-}IFN\text{-}IR^{-/-}Rag2^{-/-}$ mice were plotted with SD (n = 3–11 for each). P values were calculated between the DNase $II^{-/-}IFN\text{-}IR^{-/-}Rag2^{+/+}$ and DNase $II^{-/-}IFN\text{-}IR^{-/-}Rag2^{-/-}$, and when the value was <0.05, it is shown by *. (*B*) A section through a joint of a 12-mo-old DNase $II^{-/-}IFN\text{-}IR^{-/-}Rag2^{-/-}$ mouse stained with H&E. (Scale bar, 0.1 mm.) (*C*) The mRNA level of the indicated genes in the joints of 11–14-mo-old WT, DNase $II^{-/-}IFN\text{-}IR^{-/-}Rag2^{+/-}$, and DNase $II^{-/-}IFN\text{-}IR^{-/-}Rag2^{-/-}$ mice was quantified by real-time PCR and is expressed relative to the GAPDH mRNA level. Bars indicate the mean value. P values are shown.

We previously found that the DNase II-null mice have a high serum level of IL-18 (12), and IL-18 is implicated in various mouse models of RA (20). However, the DNase$II^{\Delta/-}IL\text{-}18^{-/-}$ mice developed arthritis with the same kinetics as the DNase$II^{\Delta/-}IL\text{-}18^{+/+}$ or DNase$II^{\Delta/-}IL\text{-}18^{+/-}$ mice (Fig. S2*A*), and the pathological changes (destruction and erosion of the cartilage and bone) (Fig. S2*B*) and the expression of MMP-3 and the inflammatory cytokine genes (TNFα, IL-1β, and IL-6) in the affected joints were similar between the DNase$II^{\Delta/-}IL\text{-}18^{-/-}$ and the DNase$II^{\Delta/-}IL\text{-}18^{+/+}$ mice (Fig. S2*C*).

Strain Independence of Arthritis in the DNase II-Null Mice. The strain background is known to affect the severity of arthritis in various mouse models (21, 22). However, when the DNase $II^{-/-}IFN\text{-}IR^{-/-}$ B6 mice were backcrossed to BALB/c mice for five generations, they developed polyarthritis with the same kinetics as the DNase $II^{-/-}IFN\text{-}IR^{-/-}$ B6 mice (Fig. S3 *A* and *B*). The MMP-3 mRNA as well as the inflammatory cytokine mRNA levels in the affected joints were similar to those in the DNase II-null B6 mice (Fig. S3*C*). The shared phenotypes of the DNase II-null mice despite the different B6 or BALB/c background indicated that heterogeneity of the MHC or other loci do not have a strong effect on the arthritis of the DNase II-null mice. The MHC-independent development of arthritis in these mice seems consistent with the dispensability of acquired immunity in this model. In other mouse models, the development of arthritis is blocked when the mice are kept in specific pathogen-free conditions (23). In contrast, DNase II-null mice develop arthritis spontaneously under the specific pathogen-free conditions, suggesting that a deficiency of the DNase II gene predicts a high risk for developing arthritis.

Therapeutic Model for Rheumatoid Arthritis. Human RA patients are treated with methotrexate (MTX) and biological agents targeted to inflammatory cytokines (TNFα, IL-1β, and IL-6) (5, 24). However, treatment with these reagents does not significantly improve established arthritis in animal models of RA such as collagen-induced arthritis (25, 26). Here, we examined the therapeutic effect of MTX, anti-IL-6 receptor, and anti-IL-1 receptor antibodies on their arthritis. When DNase $II^{-/-}IFN\text{-}IR^{-/-}$ mice showing arthritis at the age of 3.5 mo were treated everyday per os (p.o.) with MTX, the joint swelling was clearly, but transiently, reduced for 10 d (Fig. 6*A*). In contrast, the joint swelling became progressively worse in the mice treated with vehicle. Similarly, the administration of the anti-IL-6 receptor mAb (MR16-1) (27) once a week or of the anti-IL-1 receptor mAb (35F5) every 5 d blocked the joint swelling (Fig. 6 *B* and *D*). The levels of TNFα, IL-1β, and IL-6 mRNAs, particularly of IL-6, were reduced by the 1 mo treatment with the anti-IL-6 receptor or anti-IL-1 receptor Ab (Fig. 6 *C* and *E*). These results confirm that a "cytokine storm" caused by several inflammatory cytokines is responsible for the development and maintenance of arthritis, in which each cytokine activates the other's gene expression and that blocking one cytokine can quell the storm and cure the disease.

Discussion

In this report, we showed that the TNFα, IL-1β, and IL-6 genes were strongly expressed at the inflamed joints of DNase II-null mice, where they established a cytokine milieu that was highly skewed toward inflammation, a situation that is also called a cytokine storm. When the function of TNFα, IL-1β, or IL-6 was perturbed in mice with established arthritis, the levels of the TNFα, IL-1β, and IL-6 mRNAs dropped. These results indicated that the inflammatory-skewed cytokine milieu was sustained by the chronic expression of at least these three cytokines, and that each cytokine could activate the other's expression, creating a positive-feedback loop (Fig. S4). The fact that synovial cells could be activated in vitro by TNFα, IL-1β, and IL-6 to express these cytokines (Fig. S5) supports the above idea.

Lymphocytes, neutrophils, and macrophages were present in the affected joints of the DNase II-null mice. Accordingly, the expression of granulocyte colony-stimulating factor, and chemokines CCL-2, -3, -4, -7, and -20 were strongly up-regulated in the affected joints (Fig. S6, and data not shown), suggesting that

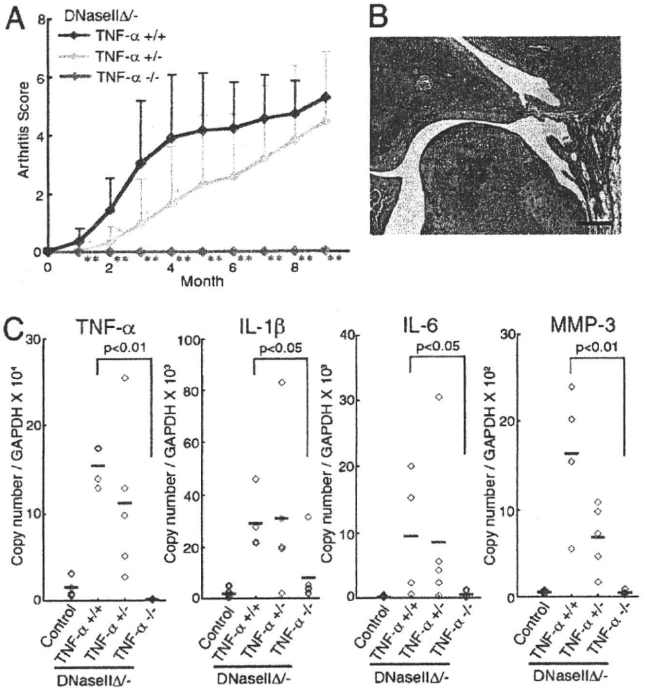

Fig. 3. TNFα-dependent arthritis. (*A*) Arthritis scores of the DNase II$^{\Delta/-}$TNFα$^{+/+}$, DNase II$^{\Delta/-}$TNFα$^{+/-}$, and DNase II$^{\Delta/-}$TNFα$^{-/-}$ mice (n = 6–9 for each) at the indicated time after poly(I):poly(C) injection, with SD. P values were calculated between the DNase II$^{\Delta/-}$TNFα$^{+/+}$ and DNase II$^{\Delta/-}$TNFα$^{-/-}$, and between the DNase II$^{\Delta/-}$TNFα$^{+/+}$ and DNase II$^{\Delta/-}$TNFα$^{+/-}$. *P = 0.01–0.05, **P < 0.01. (*B*) Section of a joint from a DNase II$^{\Delta/-}$TNFα$^{-/-}$ mouse 11 mo after poly(I):poly(C) injection, stained with H&E. (Scale bar, 0.1 mm.) (*C*) RNA from the joints of WT, DNase II$^{\Delta/-}$TNFα$^{+/+}$, DNase II$^{\Delta/-}$TNFα$^{+/-}$, or DNase II$^{\Delta/-}$TNFα$^{-/-}$ mice 9–12 mo after poly(I):poly(C) injection, was analyzed by real-time PCR for the indicated mRNA. The data are expressed relative to the GAPDH mRNA level with horizontal bars for the mean value. P values are shown.

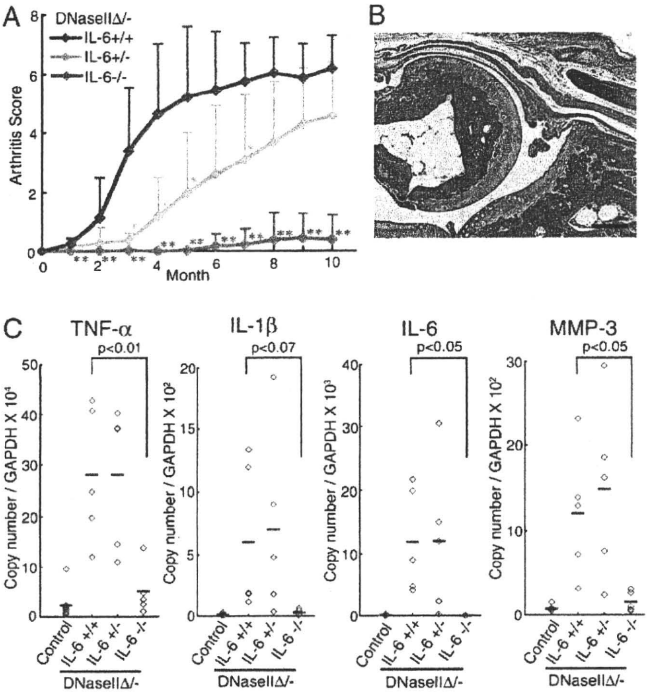

Fig. 4. IL-6–dependent arthritis. (*A*) Arthritis scores of the DNaseII$^{\Delta/-}$IL-6$^{+/+}$, DNase II$^{\Delta/-}$IL-6$^{+/-}$, and DNase II$^{\Delta/-}$IL-6 $^{-/-}$ mice (n = 5–7 per genotype) after the injection of poly(I):poly(C), plotted with SD. P values were calculated between DNase II$^{\Delta/-}$IL-6$^{+/+}$ and DNase II$^{\Delta/-}$IL-6$^{-/-}$ and between DNase II$^{\Delta/-}$IL-6$^{+/+}$ and DNase II$^{\Delta/-}$IL-6 $^{+/-}$. *P = 0.01–0.05; **P < 0.01. (*B*) A section of a joint from a DNase II$^{\Delta/-}$IL-6$^{-/-}$ mouse 11 mo after the poly(I):poly(C) injection, stained with H&E. (Scale bar, 0.1 mm.) (*C*) Real-time PCR analysis of the joint RNA from WT, DNase II$^{\Delta/-}$IL-6$^{+/+}$, DNase II$^{\Delta/-}$IL-6$^{+/-}$, and DNase II$^{\Delta/-}$IL-6$^{-/-}$ mice 11–12 mo after the poly(I):poly(C) injection for the indicated mRNA. The data are expressed relative to the GAPDH mRNA level with the mean value (bars). P values are shown.

these cytokines had recruited the lymphocytes, neutrophils, and macrophages. The expression of these cytokine and chemokine genes was completely prevented by blocking the action of TNFα, IL-1β, or IL-6. All of the pathological changes in the joints, such as the expression of MMP-3, pannus formation, and bone destruction, were also blocked when these cytokines were inhibited. These results indicate that these three cytokines play a critical role in the development of arthritis and that the inflammation-skewed cytokine milieu is fundamental for the establishment and maintenance of arthritis.

The primary defect caused by the DNase II deficiency is the macrophages' inability to digest DNA from apoptotic cells or erythroid precursor cells. In these mice, the macrophages carrying undigested DNA were present in the bone marrow and spleen and were observed even in the DNase II-null mice lacking TNFα or IL-6, which do not develop arthritis. Interestingly, the macrophages in the affected joints did not carry undigested DNA (Fig. S1*B*). Thus, a factor(s) released from the macrophages in the bone marrow, spleen, or other tissues seems to trigger the arthritis in the joint. IFNβ is expressed by macrophages carrying undigested DNA (11), but the arthritis in the DNase II-null mice develops in the IFN type I receptor-null background, indicating that type I-IFN is dispensable for the arthritis in our model. The TNFα mRNA is expressed by macrophages carrying undigested DNA in the presence or absence of lymphocytes or IL-6 (Fig. S7*A*), and a low but significant level of TNFα could be detected in the blood of the mice. Because the systemic and constitutive expression of a TNFα transgene causes arthritis in mice (28), it is likely that TNFα triggers arthritis in the DNase II-null mice. In addition, caspase 1 was activated in the macrophages carrying undigested DNA (Fig. S7*B*). Although we could not detect IL-1β or IL-6 in the serum of the DNase II-null mice, it is possible that an undetectable level of IL-1β or IL-6 produced by the macrophages triggers arthritis by stimulating synoviocytes in the joints.

There are two DNA-sensing systems in mammals that activate the innate immunity: the Toll-like receptor (TLR) system including TLR9, which recognizes bacterial DNA in lysosomes, and the TLR-independent system, which senses viral DNA in the cytosol (29). In fetal liver macrophages carrying undigested DNA, the IFNβ gene is activated in a TLR-independent manner (30). Similarly, TLR9 was dispensable for the development of arthritis in the DNase II-null mice (Fig. S8), and the TNFα gene was constitutively activated in their bone marrow (Fig. S7*A*), indicating that the undigested DNA activates the macrophages to produce TNFα in a TLR9-independent manner. Whether recently identified DNA sensors such as DAI, HMGB1, and AIM2 (31) function in the DNase II-null macrophages remains to be studied.

The DNase II-null bone marrow-derived cells were sufficient to cause arthritis, but the lymphocytes played a protective role. This finding concurs with the lymphocyte-independent arthritis reported in TNFα-transgenic mice (32), but does not explain the good therapeutic effect of lymphocyte-blocking agents in a significant population of RA patients (2, 3). RA is a heterogeneous syndrome (33). Activated CD4$^+$ T cells in SKG mice and the B cells in K/BxN TCR transgenic mice cause lymphocyte-dependent chronic arthritis (34). In both cases, however, the TNFα, IL-1, and IL-6 genes are activated in the joints, and a null mutation in any of these genes blocks the development of arthritis (15, 35), indicating that the proinflammation-skewed cytokine milieu in the joints is a common event. Activated macrophages,

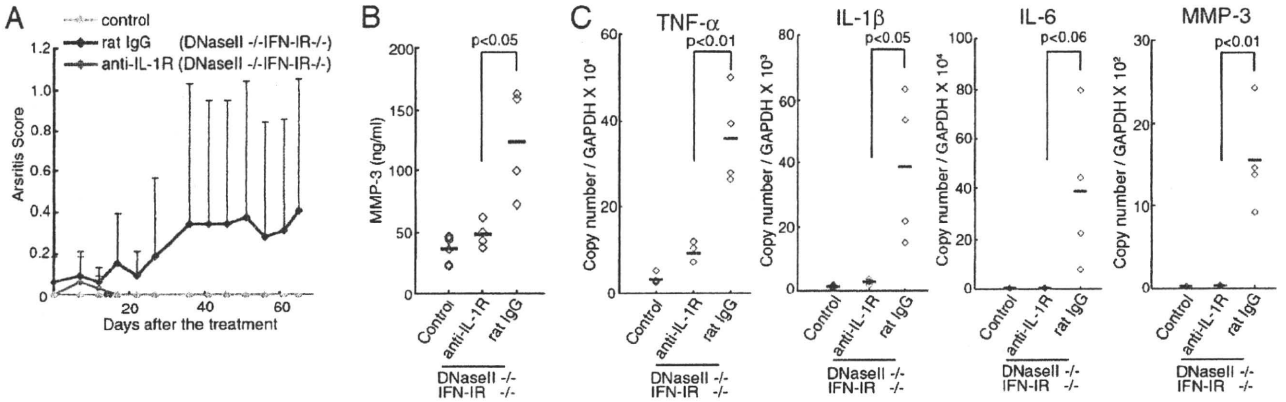

Fig. 5. IL-1β–dependent arthritis. Rat anti-IL-1R mAb or control IgG was injected into 1-mo-old DNase II$^{-/-}$IFN-IR$^{-/-}$ mice (n = 4 per group). (*A*) The arthritis scores were determined at the indicated time and are plotted with SD. (*B*) At 2.5 mo after the treatment, the serum MMP-3 level was determined. Horizontal bars indicate the mean value. The MMP-3 level of the age-matched WT littermate mice is also shown. (*C*) RNA from the joints of DNase II$^{-/-}$IFN-IR$^{-/-}$ mice treated with rat IL-1R mAb or control IgG was analyzed by real-time PCR 2.5 mo after the treatment for the indicated mRNA. Values are expressed relative to the GADPH mRNA level with horizontal bars for the mean values. Values for the joints of the age-matched WT littermate mice are also shown. *P* values are shown for *B* and *C*.

activated helper T cells, and autoimmune serum can trigger the storm. The lymphocyte-triggered arthritis would be blocked by lymphocyte-blocking agents. However, our results indicated that arthritis triggered by activated macrophages can be aggravated by lymphocytes-blocking agents. This may be similar to the previous observation that the adaptive immune system attenuates the autoimmune disease caused by the α-mannosidase-II deficiency (36). In any case, the appropriate treatment of a particular RA patient could be chosen according to whether the disease is triggered by lymphocytes or macrophages.

soJIA, also called Still's disease, constitutes about 10% of juvenile idiopathic arthritis (JIA) and is distinguished clinically from other forms of JIA by the almost equal incidence in both sexes, generalized lymphadenopathy, lack of a strong MHC association or of the involvement of acquired immunity, and a good therapeutic response to IL-1β– or IL-6–blocking agents (37, 38). A high level of IL-18 in the serum and a strong association with macrophage activation syndrome (MAS) are also characteristic of soJIA (37). These properties are observed in DNase II-null mice, supporting the idea that arthritis in DNase II-null mice is a good model of soJIA. Vastert et al. (37) proposed that soJIA is an autoinflammatory syndrome rather than a classic autoimmune disease. The pathology of arthritis of the DNase II-null mice fully agrees with this idea. Arthritis in the DNase II-null mice is caused

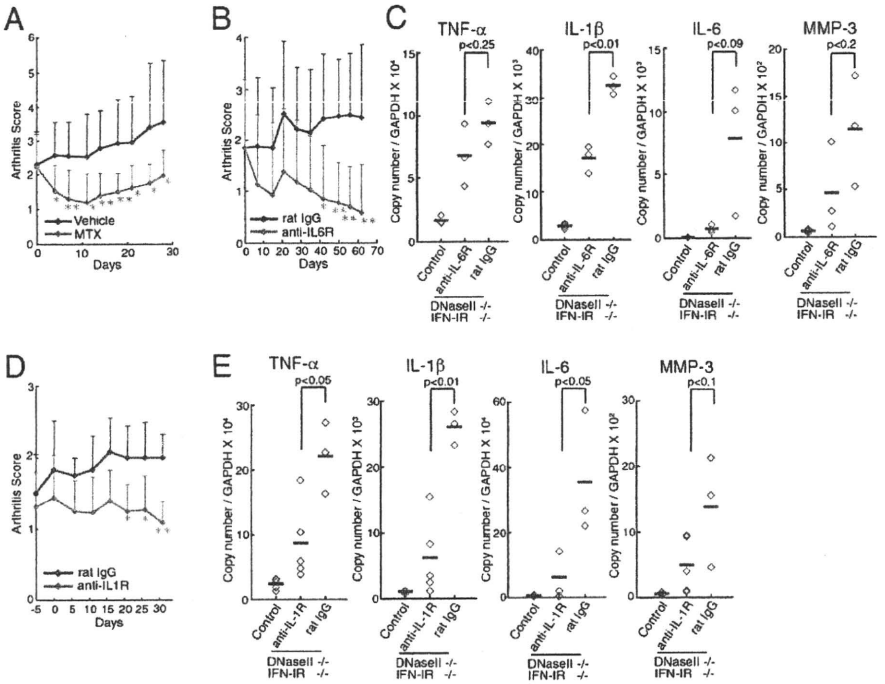

Fig. 6. Therapeutic effect of MTX, anti-IL-6R, and anti-IL-1R treatments. The DNase II$^{-/-}$IFN-IR$^{-/-}$ mice (3.5–13 mo old) with affected joints were treated with MTX (n = 9–10 for each group) (*A*), anti-IL-6R (n = 9–10 for each group) (*B* and *C*), or anti-IL-1R mAb (n = 3–6 for each group) (*D* and *E*), and arthritis scores for the indicated mice are plotted with SD. After a 4-wk treatment with anti-IL-6R mAb (*C*) or anti-IL-1R mAb (*E*), the indicated mRNA level in the joints was quantified by real-time PCR and shown relative to the GAPDH mRNA. The mean value is indicated (bars). RNA from the age-matched littermate control mice was also analyzed. *P* values were calculated. In *A*, *B*, and *D*, $*P$ = 0.01–0.05; $**P < 0.01$.

by the activation of macrophages, due to the defect in DNA degradation. It is possible that the activation of macrophages is also the first event in soJIA. Functional soJIA-specific SNPs have been reported in IL-6 and macrophage migration inhibitory factor (MIF) (39, 40). Our results indicate that the chronic activation of macrophages owing to the lack of lysosomal enzymes or by other causes can lead to autoinflammatory syndromes like soJIA, and it will be interesting to learn whether mutation in lysosomal enzymes can be found in the soJIA patients. In any case, DNase II-null mice will contribute to our understanding of RA, particularly soJIA.

Materials and Methods

Mice. The mice are described in *SI Materials and Methods*. The pathological phenotypes were compared between different genotypes using littermates or mice kept in a closed colony. Mice were housed in a specific pathogen-free facility at Kyoto University Graduate School of Medicine, Oriental Bioservices, and Chugai Pharmaceutical. All animal experiments were carried out in accordance with protocols approved by the Animal Care and Use Committee at Kyoto University Graduate School of Medicine and Chugai Pharmaceutical.

Bone Marrow Transplantation. Bone marrow cells ($CD45.2^+$) were collected from a 2-mo-old DNase $II^{\Delta/-}$ or control mouse and injected i.v. into four 1-mo-old recipient mice ($CD45.1^+$) treated with γ-ray (10 G). The mice received drinking water containing 1 mg/mL neomycin and ampicillin for 1 mo. The replacement of blood cells was confirmed by FACS analysis for CD45.1 or CD45.2.

Treatment with MTX and Monoclonal Antibodies. MTX was administered p.o. daily at 3 mg/g body weight. Rat anti-IL-1 receptor mAb (35F5) (19) was administered i.v. at 27 μg/g body weight, followed by i.p. injection every 5 d at 13 μg/g body weight. Rat anti-IL-6R mAb (MR16-1) (27) was administered i.v. at 100 μg/g body weight, followed by i.p. injection at 25 μg/g body weight once a week. Normal rat IgG (Cappel) was administered as a control. Four days or more after the last injection, the blood and joints were collected.

Clinical Assessment and Histology. Swelling of the fore and hind limb was manually inspected and scored: 0, no; 0.25, faint; 0.5, mild; 1, severe swelling or deformation. The digits and paw of each limb were assessed separately. The scores were summed, and a total score (maximum 8 per mouse) was assigned. To prepare paraffin sections, tissues were fixed with 4% paraformaldehyde in 0.1 M sodium phosphate buffer (pH 7.2) containing 4% sucrose or with 8% formaldehyde and embedded in paraffin. Joints were incubated at room temperature for 24 h in Morse's solution (10% sodium citrate and 22.5% formic acid) for decalcification before the paraffinization. The blocks were sectioned at 2–4 μm, deparaffinized, and stained with H&E.

Statistical Analysis. Two-tailed Student's *t* tests were used for statistical testing between two groups.

ACKNOWLEDGMENTS. We thank A. Hicks (Roche, Nutley, NJ) for 35F5 mAb, S. Akira (Osaka University, Osaka) for $TLR9^{-/-}$ mice, Y. Shinkai (Kyoto University, Kyoto) for $Rag2^{-/-}$ mice, K. Sekikawa (National Institute of Agrobiological Sciences, Nishinomiya, Japan) for $TNF\alpha^{-/-}$ mice, K. Nakanishi and H. Tsutsui (Hyogo College of Medicine) for $IL\text{-}18^{-/-}$ mice, and M. Kopf (Eidgenössische Technische Hochschule, Zurich) for $IL\text{-}6^{-/-}$ mice. We thank K. Miwa and M. Ohtani for help at the initial stages of this work, M. Nishihara for help in MTX experiments, and T. Fujimoto and K. Ishihara (Kawasaki Medical School) for advice. We thank M. Fujii and M. Harayama for secretarial assistance. This work was supported in part by grants-in-aid from the Ministry of Education, Science, Sports, and Culture in Japan.

1. Firestein GS (2003) Evolving concepts of rheumatoid arthritis. *Nature* 423:356–361.
2. Cope AP (2008) T cells in rheumatoid arthritis. *Arthritis Res Ther* 10(Suppl 1):S1.
3. Tedder TF (2009) CD19: A promising B cell target for rheumatoid arthritis. *Nat Rev Rheumatol* 5:572–577.
4. Kinne RW, Bräuer R, Stuhlmüller B, Palombo-Kinne E, Burmester GR (2000) Macrophages in rheumatoid arthritis. *Arthritis Res* 2:189–202.
5. Feldmann M, Maini SR (2008) Role of cytokines in rheumatoid arthritis: An education in pathophysiology and therapeutics. *Immunol Rev* 223:7–19.
6. Nagata S (2005) DNA degradation in development and programmed cell death. *Annu Rev Immunol* 23:853–875.
7. Nagata S, Hanayama R, Kawane K (2010) Autoimmunity and the clearance of dead cells. *Cell* 140:619–630.
8. Evans CJ, Aguilera RJ (2003) DNase II: Genes, enzymes and function. *Gene* 322:1–15.
9. Kawane K, et al. (2001) Requirement of DNase II for definitive erythropoiesis in the mouse fetal liver. *Science* 292:1546–1549.
10. Kawane K, et al. (2003) Impaired thymic development in mouse embryos deficient in apoptotic DNA degradation. *Nat Immunol* 4:138–144.
11. Yoshida H, Okabe Y, Kawane K, Fukuyama H, Nagata S (2005) Lethal anemia caused by interferon-beta produced in mouse embryos carrying undigested DNA. *Nat Immunol* 6:49–56.
12. Kawane K, et al. (2006) Chronic polyarthritis caused by mammalian DNA that escapes from degradation in macrophages. *Nature* 443:998–1002.
13. Young-Min S, et al. (2007) Biomarkers predict radiographic progression in early rheumatoid arthritis and perform well compared with traditional markers. *Arthritis Rheum* 56:3236–3247.
14. Asadullah K, Sterry W, Volk HD (2003) Interleukin-10 therapy—review of a new approach. *Pharmacol Rev* 55:241–269.
15. Hata H, et al. (2004) Distinct contribution of IL-6, TNF-alpha, IL-1, and IL-10 to T cell-mediated spontaneous autoimmune arthritis in mice. *J Clin Invest* 114:582–588.
16. van den Berg WB, Miossec P (2009) IL-17 as a future therapeutic target for rheumatoid arthritis. *Nat Rev Rheumatol* 5:549–553.
17. Ishigame H, et al. (2009) Differential roles of interleukin-17A and -17F in host defense against mucoepithelial bacterial infection and allergic responses. *Immunity* 30: 108–119.
18. Kishimoto T (2005) Interleukin-6: From basic science to medicine—40 years in immunology. *Annu Rev Immunol* 23:1–21.
19. Chizzonite R, et al. (1989) Two high-affinity interleukin 1 receptors represent separate gene products. *Proc Natl Acad Sci USA* 86:8029–8033.
20. Wei XQ, Leung BP, Arthur HM, McInnes IB, Liew FY (2001) Reduced incidence and severity of collagen-induced arthritis in mice lacking IL-18. *J Immunol* 166:517–521.
21. Horai R, et al. (2000) Development of chronic inflammatory arthropathy resembling rheumatoid arthritis in interleukin 1 receptor antagonist-deficient mice. *J Exp Med* 191:313–320.
22. Phillips K, Kedersha N, Shen L, Blackshear PJ, Anderson P (2004) Arthritis suppressor genes TIA-1 and TTP dampen the expression of tumor necrosis factor alpha, cyclooxygenase 2, and inflammatory arthritis. *Proc Natl Acad Sci USA* 101:2011–2016.
23. Yoshitomi H, et al. (2005) A role for fungal beta-glucans and their receptor Dectin-1 in the induction of autoimmune arthritis in genetically susceptible mice. *J Exp Med* 201: 949–960.
24. van Vollenhoven RF (2009) Treatment of rheumatoid arthritis: State of the art 2009. *Nat Rev Rheumatol* 5:531–541.
25. Takagi N, et al. (1998) Blockage of interleukin-6 receptor ameliorates joint disease in murine collagen-induced arthritis. *Arthritis Rheum* 41:2117–2121.
26. Fiehn C, Kratz F, Sass G, Müller-Ladner U, Neumann E (2008) Targeted drug delivery by in vivo coupling to endogenous albumin: An albumin-binding prodrug of methotrexate (MTX) is better than MTX in the treatment of murine collagen-induced arthritis. *Ann Rheum Dis* 67:1188–1191.
27. Okazaki M, Yamada Y, Nishimoto N, Yoshizaki K, Mihara M (2002) Characterization of anti-mouse interleukin-6 receptor antibody. *Immunol Lett* 84:231–240.
28. Keffer J, et al. (1991) Transgenic mice expressing human tumour necrosis factor: A predictive genetic model of arthritis. *EMBO J* 10:4025–4031.
29. Takeuchi O, Akira S (2010) Pattern recognition receptors and inflammation. *Cell* 140: 805–820.
30. Okabe Y, Kawane K, Akira S, Taniguchi T, Nagata S (2005) Toll-like receptor-independent gene induction program activated by mammalian DNA escaped from apoptotic DNA degradation. *J Exp Med* 202:1333–1339.
31. Hornung V, Latz E (2010) Intracellular DNA recognition. *Nat Rev Immunol* 10: 123–130.
32. Kontoyiannis D, Pasparakis M, Pizarro TT, Cominelli F, Kollias G (1999) Impaired on/off regulation of TNF biosynthesis in mice lacking TNF AU-rich elements: Implications for joint and gut-associated immunopathologies. *Immunity* 10:387–398.
33. Kochi Y, Suzuki A, Yamada R, Yamamoto K (2009) Genetics of rheumatoid arthritis: Underlying evidence of ethnic differences. *J Autoimmun* 32:158–162.
34. Benoist C, Mathis D (2000) A revival of the B cell paradigm for rheumatoid arthritis pathogenesis? *Arthritis Res* 2:90–94.
35. Ji H, et al. (2002) Critical roles for interleukin 1 and tumor necrosis factor alpha in antibody-induced arthritis. *J Exp Med* 196:77–85.
36. Green RS, et al. (2007) Mammalian N-glycan branching protects against innate immune self-recognition and inflammation in autoimmune disease pathogenesis. *Immunity* 27:308–320.
37. Vastert SJ, Kuis W, Grom AA (2009) Systemic JIA: New developments in the understanding of the pathophysiology and therapy. *Best Pract Res Clin Rheumatol* 23:655–664.
38. Yokota S, et al. (2005) Therapeutic efficacy of humanized recombinant anti-interleukin-6 receptor antibody in children with systemic-onset juvenile idiopathic arthritis. *Arthritis Rheum* 52:818–825.
39. Fishman D, et al. (1998) The effect of novel polymorphisms in the interleukin-6 (IL-6) gene on IL-6 transcription and plasma IL-6 levels, and an association with systemic-onset juvenile chronic arthritis. *J Clin Invest* 102:1369–1376.
40. Donn R, et al. (2002) Mutation screening of the macrophage migration inhibitory factor gene: Positive association of a functional polymorphism of macrophage migration inhibitory factor with juvenile idiopathic arthritis. *Arthritis Rheum* 46:2402–2409.

Cell

Autoimmunity and the Clearance of Dead Cells

Shigekazu Nagata,[1,2,*] Rikinari Hanayama,[1,2] and Kohki Kawane[1,2]
[1]Department of Medical Chemistry, Graduate School of Medicine, Kyoto University, Yoshida-Konoe, Sakyo, Kyoto 606-8501, Japan
[2]Core Research for Evolutional Science and Technology, Japan Science and Technology Corporation, Yoshida-Konoe, Sakyo, Kyoto 606-8501, Japan
*Correspondence: snagata@mfour.med.kyoto-u.ac.jp
DOI 10.1016/j.cell.2010.02.014

To maintain organismal homeostasis, phagocytes engulf dead cells, which are recognized as dead by virtue of a characteristic "eat me" signal exposed on their surface. The dead cells are then transferred to lysosomes, where their cellular components are degraded for reuse. Inefficient engulfment of dead cells activates the immune system, causing disease such as systemic lupus erythematosus, and if the DNA of the dead cells is not properly degraded, the innate immune response becomes activated, leading to severe anemia and chronic arthritis. Here, we discuss how the endogenous components of dead cells activate the immune system through both extracellular and intracellular pathways.

Introduction

In the Japanese movie *Departures* (*Okuribito* in Japanese), which won the 2009 Oscar for best foreign language film, death is regarded as a gate. The deceased are gently washed, dressed, and placed in a coffin for departure into the next life. Similarly, when the cells in our bodies die, an elaborate process takes place to remove them and to give them a new life by using their components.

Many extra cells are generated and die during animal development. In human adults, billions of cells die every day as part of the body's natural processes. Cells that become damaged by microbial infection or mechanical stress also die. The cell death that occurs in the physiological setting is programmed, and is therefore called programmed cell death (Lockshin and Zakeri, 2001). Apoptosis is the major death process, but necrosis and autophagic cell death have also been proposed to play roles in programmed cell death (Kroemer et al., 2009). Dying cells secrete a "find me" signal, and they expose an "eat me" signal on their surface. In response to the "find me" signal, macrophages approach the dead cells; they then recognize the "eat me" signal (Ravichandran and Lorenz, 2007). Using sophisticated cell machinery, the phagocytes ingest the dead cells, direct them to lysosomes, and degrade their cellular components into basic biochemical building blocks: amino acids, nucleotides, fatty acids, and monosaccharides. These molecules will be released from the lysosomes and reused to make new macromolecules. In definitive erythropoiesis, the process by which red blood cells are generated, the nuclei are extruded from erythroid precursor cells at the final differentiation stage and are engulfed by macrophages (Chasis and Mohandas, 2008). The machinery used for the engulfment and degradation of the extruded nuclei appears similar to that used for the removal of apoptotic cells.

Mice deficient in the engulfment of apoptotic cells develop systemic lupus erythematosus (SLE)-type autoimmune diseases (Hanayama et al., 2004). A defect in the degradation of the chromosomal DNA from engulfed cells in mice activates macrophages, leading to lethal anemia in embryos and chronic arthritis in adults (Kawane et al., 2001; Kawane et al., 2006). These observations indicate that dead cells and the nuclei expelled from erythroid precursor cells need to be swiftly cleared for animals to maintain homeostasis.

Programmed Cell Death

Based on morphological and biochemical criteria, four different cell-death processes (apoptosis, cornification, necrosis, and autophagy) have been officially proposed (Kroemer et al., 2009). In apoptosis, the cell and nuclei condense and become fragmented and are engulfed by phagocytes (Kerr et al., 1972). Apoptosis is regulated by gene products, and programmed cell death has often been used synonymously with apoptosis. However, necrosis is also regulated by gene products (Cho et al., 2009; He et al., 2009), and it may be preferable to use the term programmed cell death in only its more general sense, that is, to refer to any cell-death process that is programmed into animal development.

It is unclear to what extent the other proposed forms of cell death can be classified as programmed cell death. Of them, autophagy, in which organelles and macromolecules are trapped by the cell's own membranes and degraded in its lysosomes, is a process by which cells survive in starvation conditions (Ohsumi, 2001). Autophagy has been proposed as a cell-death process because cells undergoing severe or prolonged autophagy may die, and dying cells often show a characteristic, autophagic morphology (Tsujimoto and Shimizu, 2005). However, there are no convincing data supporting the notion that autophagy kills the cells, and hence the term autophagic cell death may be misleading (Kroemer and Levine, 2008). Cornification, a cell-differentiation process, describes the cell death that occurs at the final step in the natural differentiation of skin cells (Lippens et al., 2005). Simi-

larly, the differentiation of the lens epithelial cells of the eye to fiber cells is accompanied by the degradation of nuclei, mitochondria, and endoplasmic reticulum (Bassnett, 2002), which can also be regarded as a cell-death process. However, it may not be appropriate to classify this cell-differentiation process as programmed cell death. In addition, although necrosis is mediated by gene products, it occurs only when apoptosis is blocked or when cells receive strong death signals under pathological conditions. Thus, we believe that apoptosis accounts for most of the physiological cell death during animal development and in the cell turnover that occurs daily.

Apoptosis

Apoptosis is activated by two pathways, the intrinsic and extrinsic pathways (Ow et al., 2008). In the intrinsic pathway, which operates in developmentally controlled and genotoxic agent-mediated apoptosis, BH3-only members of the Bcl-2 family are transcriptionally upregulated and stimulate the release of cytochrome C from the mitochondria. Together with Apaf-1, cytochrome C activates caspase 9, which leads to the activation of downstream caspases, including caspases 3 and 7. The antiapoptotic members of the Bcl-2 family inhibit the release of cytochrome C from mitochondria by a mechanism that has not been well elucidated. This intrinsic pathway is thought to be well conserved in metazoans, but its key step, the release of cytochrome C from mitochondria, is not observed in the nematode *C. elegans* or in the fruit fly *Drosophila* (Oberst et al., 2008).

Fas ligand (FasL), tumor necrosis factor (TNF), and TRAIL (TNF-related apoptosis-inducing ligand) are type II membrane proteins that can activate the extrinsic death pathway (Krammer, 2000; Nagata, 1997; Strasser et al., 2009). The binding of FasL to its receptor (Fas) induces the formation of the death-inducing signaling complex (DISC), consisting of Fas, an adaptor protein (FADD), and procaspase 8. Formation of the DISC leads to the processing and activation of caspase 8. Depending on the cell type, there are two pathways that can be activated downstream of caspase 8. In type I cells (for example, thymocytes), caspase 8 directly activates caspase 3 to kill the cells; in type II cells (hepatocytes), caspase 8 cleaves Bid, a BH3-only member of the Bcl-2 family, and the cleaved Bid (tBid) induces the release of cytochrome C from the mitochondria, which leads to the activation of the caspase 9-caspase 3 pathway.

In both the intrinsic and extrinsic pathways, apoptosis is completed by the cleavage of a set of cellular proteins (more than 500 substrates) by effector caspases (caspases 3 and 7) (Lüthi and Martin, 2007; Timmer and Salvesen, 2007) (http://cutdb.burnham.org/; http://bioinf.gen.tcd.ie/casbah/). The massive protein cleavage is probably responsible for the morphological and biochemical changes that occur during apoptosis, and for killing the cells. However, with a few exceptions (see below), the physiological meaning of the specific cleavage events is not clear. In addition to killing the cells, caspase activation is involved in the cells' production of the "find me" and "eat me" signals sensed by phagocytes.

Apoptotic DNA Degradation and Membrane Blebbing

One of notable hallmarks of apoptosis is DNA fragmentation, the cleavage of chromosomal DNA into 180 bp nucleosomal units (Wyllie, 1980). This process, accomplished by CAD (caspase-activated DNase), also called DFF-40 (DNA fragmentation factor 40), is the most representative example of how caspase activation causes a characteristic feature of apoptosis (Enari et al., 1998; Liu et al., 1997). In healthy cells, CAD is complexed with its inhibitor, ICAD (inhibitor of CAD), also called DFF-45 (Enari et al., 1998; Liu et al., 1997; Sakahira et al., 1998), which also acts as a chaperone for CAD to ensure its correct folding (Sakahira et al., 2000). Caspase 3 cleaves ICAD at two positions (Sakahira et al., 1998), which allows CAD to form a homodimer that has a scissor-like structure (Woo et al., 2004). CAD carries a nuclear-localization signal and cleaves DNA in the nucleus via specific histidine residues (Sakahira et al., 2001) located in the deep cleft between the "blades" of the "scissors." This structure prevents CAD from accessing the DNA on nucleosomes, but allows it access to DNA in the spacer regions between them, which explains why the chromosomal DNA is degraded into nucleosomal units during apoptotic cell death. CAD generates DNA fragments with a 3′-hydroxyl group. This group is identified by TUNEL (terminal transferase-mediated dUTP nick end labeling) staining, which is widely used to detect apoptotic cells in vitro and in vivo. At the early stage of apoptosis, DNA is degraded into relatively large pieces (50–200 kb). Endonucleases other than CAD have been postulated to perform this cleavage (Samejima et al., 2001; Susin et al., 2000). However, at least in our hands, no DNA degradation (whether to high-molecular-weight fragments or nucleosomal units) can be observed in cells lacking CAD (Kawane et al., 2003), indicating that other nucleases are not involved or play only a limited role.

Caspase cleavage also explains another hallmark of apoptotis, membrane blebbing. ROCK1 (Rho-associated kinase 1), a substrate of caspase 3, phosphorylates various cytoskeletal proteins, including myosin light chain, and regulates the actin cytoskeleton. ROCK1 is normally regulated by Rho GTPase, but its cleavage by caspase 3 removes its regulatory domain and renders it constitutively active (Coleman et al., 2001; Sebbagh et al., 2001). This aberrantly activated ROCK1 intensively phosphorylates myosin light chain, leading to membrane blebbing.

The microinjection of active CAD into cells causes DNA fragmentation and quickly kills the cells (Susin et al., 2000). In contrast, CAD-deficient cells are efficiently killed by apoptotic stimuli without DNA degradation (Kawane et al., 2003). As described above, given that many proteins and enzymes essential for cell survival are cleaved and inactivated by caspases, it is likely that once caspases are activated by apoptotic stimuli, there are many ways to kill the cells.

Engulfment of Apoptotic Cells

When apoptotic cells are left on a Petri dish for a long time, their plasma membrane ruptures and cellular contents are released, in a process called secondary necrosis (Kerr et al., 1972). On the other hand, apoptotic cells in vivo are quickly recognized by phagocytes and engulfed to prevent the release of their intracellular materials, which can be immunogenic. For the specific and efficient engulfment of apoptotic cells, the dead cells discharge molecules to

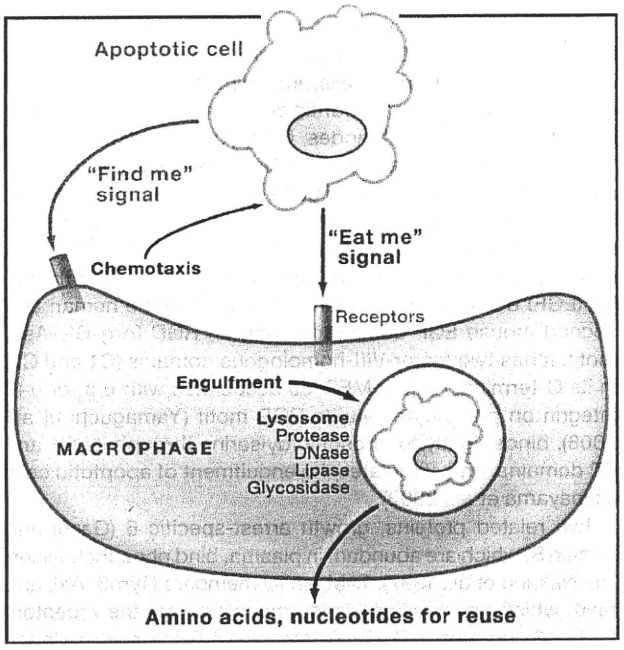

Figure 1. Engulfment of Apoptotic Cells by Macrophages
When cells undergo apoptosis, they release "find me" signals to recruit macrophages, and expose "eat me" signals on their surface. In response to the "find me" signal, macrophages approach the dead cells, and they engulf them by recognizing the "eat me" signal. The engulfed dead cells are transferred to lysosomes, where all their components are degraded into amino acids, nucleotides, fatty acids, and monosaccharides by lysosomal enzymes.

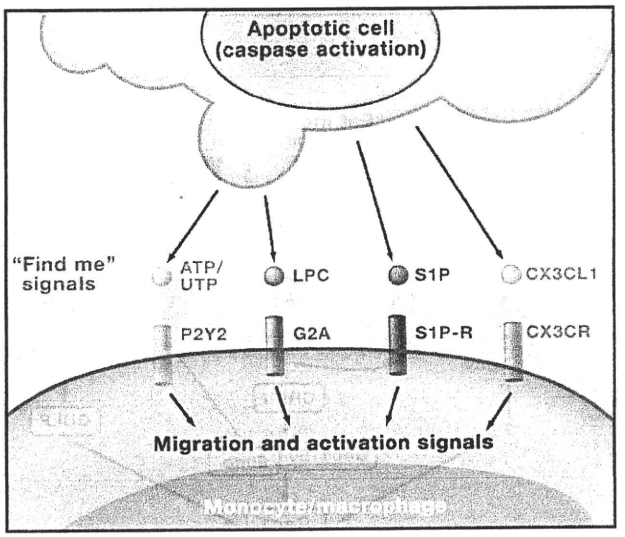

Figure 2. Proposed "Find Me" Signals
As "find me" signals, ATP/UTP, lysophosphatidylcholine (LPC), sphingosine-1-phosphate (S1P), and fractalkine CX3CL1 have been proposed. These molecules bind specific receptors on macrophages, all of which are G protein-coupled seven-transmembrane receptors, and activate them for chemotaxis.

recruit phagocytes ("find me" signals), and they expose on their surface molecules that are recognized by phagocytes ("eat me" signals) (Figure 1).

"Find Me" Signals

By assaying the ability of the culture supernatant from apoptotic cells to trigger the chemotaxis of macrophages, Lauber et al. (2003) identified lysophosphatidylcholine (LPC) as a "find me" signal (Figure 2). It is released from apoptotic cells by the caspase-3-dependent activation of phospholipase A2, which converts phosphatidylcholine to LPC. The binding of LPC to G2A (G2 accumulation protein or G protein-coupled receptor 132) activates macrophages to undergo chemotaxis (Peter et al., 2008). This model is attractive, but the concentration of LPC required to cause the chemotaxis of phagocytes is rather high (20–30 μM) and may not be reached physiologically.

Two other molecules, sphingosine-1-phosphate (S1P) and CX3CL1/fractalkine, have also been proposed to act as "find me" signals (Gude et al., 2008; Truman et al., 2008). S1P is produced by sphingosine kinase in a caspase-dependent manner and secreted from apoptotic cells; it stimulates the chemotaxis of macrophages by binding its specific receptor, S1P-R. Fractalkine, CX3CL1, is synthesized as a membrane-associated protein, rapidly processed, and released from apoptotic neurons or B cells. It activates microglia and macrophages to undergo chemotaxis by binding to its receptor, CX3CR. In addition, ATP and UTP released from apoptotic cells in a caspase-dependent manner have recently been shown to act as "find me" signals for apoptotic cells (Elliott et al., 2009). Whether these proposed "find me" signals are redundant, additive, or synergistic remains to be studied.

Apoptotic cells appear to mostly (or exclusively) recruit macrophages (Truman et al., 2004). Yet, the proposed molecules (LPC, S1P, and ATP/UTP) activate not only macrophages but also neutrophils and lymphocytes (Florey and Haskard, 2009; Lecut et al., 2009). Bournazou et al. (2009) propose that lactoferrin is synthesized in apoptotic cells, secreted, and inhibits the migration of neutrophils. However, this may not be consistent with the quick killing of the death-factor-induced apoptosis that does not require protein synthesis. An involvement of lactoferrin in the "find me" process should be clarified with the lactoferrin-deficient mice (Ward et al., 2003).

"Eat Me" Signals

Macrophages engulf dead cells but not healthy ones, indicating either that dying cells expose "eat me" signals recognized by phagocytes or that healthy cells display "don't eat me" signals. The best-studied "eat me" signal is phosphatidylserine, a component of the cell plasma membrane that is kept exclusively on the inner leaflet of the lipid bilayer in healthy cells (Balasubramanian and Schroit, 2003). Phosphatidylserine is exposed on the cell surface when cells undergo apoptosis (Fadok et al., 1992). Moreover, when phosphatidylserine is inserted into the plasma membrane of erythrocytes, they are recognized and engulfed by macrophages (Tanaka and Schroit, 1983). Furthermore, the masking of phosphatidylserine inhibits the engulfment of apoptotic cells in vitro and in vivo (Asano et al., 2004; Krahling et al., 1999). These results strongly point to phosphatidylserine as the most likely candidate for the "eat me" signal.

The exposure of phosphatidylserine on the surface of apoptotic cells is found not only in mammals but also in *Drosophila* and *C. elegans* (van den Eijnde et al., 1998; Venegas and Zhou,

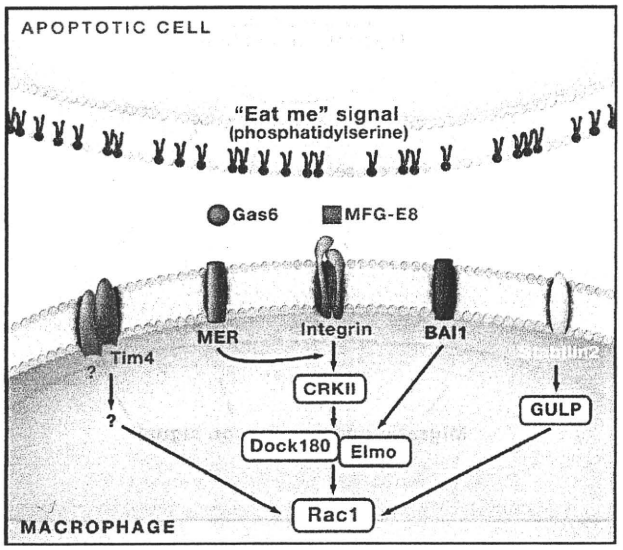

Figure 3. Molecules Proposed to Recognize Phosphatidylserine
The most likely "eat me" signal is phosphatidylserine. MFG-E8 and Gas6 are secreted proteins that bind phosphatidylserine and work as bridging molecules between apoptotic cells and macrophages. Tim-4, BAI1, and Stabilin-2 are type I-membrane proteins that are proposed phosphatidylserine receptors. Molecules that activate Rac1 (CrkII, Dock180, Elmo, and GULP) are involved in the engulfment of apoptotic cells.

2007). This process is caspase dependent (Martin et al., 1996), but how caspase activity leads to the cell-surface exposure of phosphatidylserine remains unsettled (Schlegel and Williamson, 2007). In one model, ATP-dependent translocases that maintain phosphatidylserine at the inner leaflet of the plasma membrane are inactivated in apoptotic cells, but Ca^{2+}-dependent phospholipid scamblase is activated, causing randomization of the membrane leaflet components (Balasubramanian and Schroit, 2003; Sahu et al., 2007). This model has been examined in mammals and *C. elegans*, but with controversial results (Darland-Ransom et al., 2008; Züllig et al., 2007).

CD47, also called integrin-associated protein (IAP), is a membrane protein with five membrane-spanning regions. When CD47-deficient red blood cells are injected into mice, they are more rapidly cleared by macrophages in the spleen than are CD47-positive cells. Oldenborg et al. (2000) therefore proposed that CD47 serves as a "don't eat me" signal. However, when CD47-positive red blood cells are loaded with phosphatidylserine, they are efficiently engulfed by macrophages (Tanaka and Schroit, 1983). Thymocytes express abundant CD47. When they undergo apoptosis, their CD47 expression is not lost, yet the apoptotic thymocytes are still efficiently engulfed by macrophages (Tada et al., 2003). These observations indicate that the "eat me" signal can overcome the "don't eat me" signal.

Bridging Molecules that Recognize Phosphatidylserine

Several secreted proteins have been identified as molecules that recognize the phosphatidylserine on apoptotic cells and promote their engulfment (Figure 3). Milk fat globule EGF factor 8 (MFG-E8), originally found associated with milk fat globules in mammary glands, is a secreted protein present on a subset of phagocytes that actively engulf apoptotic cells (Hanayama et al., 2002). It is expressed by macrophages and immature dendritic cells, including tingible-body macrophages and follicular dendritic cells at the germinal centers in the spleen and lymph nodes, thioglycollate-elicited peritoneal macrophages, granulocyte-macrophage colony stimulating factor (GM-CSF)-induced bone marrow-derived immature dendritic cells, and Langerhans cells in the skin (Hanayama et al., 2004; Kranich et al., 2008; Miyasaka et al., 2004). MFG-E8 contains one (human) or two (mouse) epidermal growth factor (EGF) domains in its N-terminal half, with the human and second mouse EGF domain carrying an RGD (Arg-Gly-Asp) motif. It has two factor-VIII-homologous domains (C1 and C2) in its C-terminal region. MFG-E8 associates with $\alpha_v\beta_3$ or $\alpha_v\beta_5$ integrin on phagocytes via its RGD motif (Yamaguchi et al., 2008), binds tightly to phosphatidylserine through its C1 and C2 domains, and stimulates the engulfment of apoptotic cells (Hanayama et al., 2002).

Two related proteins, growth arrest-specific 6 (Gas6) and protein S, which are abundant in plasma, bind phosphatidylserine (Nakano et al., 1997). TAM family members (Tyro3, Axl, and Mer), which are tyrosine-kinase receptors, are the receptors for Gas6 and protein S. Gas6 and protein S are involved in the vitamin K-dependent clotting system, and a deficiency in Gas6 or its receptor causes platelet dysfunction (Angelillo-Scherrer et al., 2005; Angelillo-Scherrer et al., 2001). On the other hand, mice expressing a kinase-dead mutant of Mer (Mer^{KD}) develop SLE-like autoimmunity (Scott et al., 2001), and the Gas6-TAM system has been proposed to play a role in the engulfment of apoptotic cells, particularly in the testis and retina (Prasad et al., 2006; Xiong et al., 2008). A recent report indicates that TAM receptors negatively regulate the innate immune reaction, and a lack of TAM receptors causes dendritic cells to overproduce interleukin-6 (IL-6), interferon (IFN), and TNFα (Rothlin et al., 2007). Given that SLE-type autoimmunity is regulated by cytokines, this overproduction of cytokines by dendritic cells might be responsible for the SLE-like autoimmunity found in the MER^{KD} mice (Scott et al., 2001).

Phosphatidylserine Receptors

Whether macrophages directly recognize apoptotic cells has been difficult to elucidate. A protein initially identified by Fadok et al. (2000) as a phosphatidylserine receptor (and consequently named PSR) is now reported to have a different function. Fadok et al. identified PSR by screening a phage-display library with a monoclonal antibody that inhibits the engulfment of apoptotic cells. Several groups subsequently reported that the deficiency of PSR causes the impaired engulfment of apoptotic cells, resulting in embryonic lethality in the mouse (Kunisaki et al., 2004; Li et al., 2003) and delayed engulfment of apoptotic cells in *C. elegans* (Wang et al., 2003). In contrast, Böse et al. (2004) who independently established *PSR* knockout mice, reported that PSR is not the protein recognized by the monoclonal antibody used by Fadok et al., and that PSR null macrophages have no defect in the engulfment of apoptotic cells. Subsequent reports have indicated that PSR is a chromatin-remodeling factor called Jumonji domain-containing 6 protein (JMJD6), which is present in the nucleus (Chang et al., 2007). Hence, the increased number of unengulfed apop-

Table 1. Molecules Involved in the Engulfment of Apoptotic Cells

C. elegans	Mammalian	Properties
CED-1	MEGF10	Type I membrane protein with multiple epidermal growth factor (EGF)-like domains in the extracellular region
CED-2	CrkII	Cytoplasmic protein with a Src homology 2 (SH2) and an SH3 domain, that functions as an adaptor for signal transduction
CED-5	Dock180	Cytoplasmic protein containing an SH3 domain; it associates with CrkII and ELMO, and activates the Rho family GTPase Rac1 as a guanine exchange factor
CED-6	GULP	Cytoplasmic protein with a phosphotyrosine-binding domain (PTB) and four SH3-binding motifs; it binds to CED-1 and functions upstream of CED-10
CED-7	ABC transporter	Protein with two homologous repeats, each harboring six transmembrane segments and one ATP-binding site
CED-10	Rac1	Small GTP-binding protein of the Ras superfamily
CED-12	ELMO	Cytoplasmic protein; it associates with CrkII and Dock180, and activates Rac1

totic cells in the animals lacking PSR may be due to increased cell death caused by the lack of JMJD6's chromatin remodeling function.

In investigating the mechanism by which macrophages that do not express MFG-E8 engulf apoptotic cells, we reported that type I membrane proteins called T cell immunoglobulin- and mucin-domain-containing molecule 4 (Tim-4) and Tim-1 serve as phosphatidylserine receptors (Miyanishi et al., 2007) (Figure 3). Tim-1 and Tim-4 consist of a signal sequence, an immunoglobulin V (IgV) domain, a mucin-like domain, a transmembrane domain, and a cytoplasmic region. They specifically bind phosphatidylserine with high affinity via their IgV domain. When Tim-1 or Tim-4 is expressed in mouse fibroblasts (NIH 3T3), which do not normally express Tim family members, the transformants efficiently engulf apoptotic cells. The short cytoplasmic region of Tim-4 is dispensable for the engulfment (Park et al., 2009) (M. Murai, M. Miyanishi, and S.N., unpublished data), indicating that Tim-4 associates with endogenous molecules on the fibroblast membrane to activate the engulfment signal. Among other Tim family members, Tim-3 also binds phosphatidylserine and stimulates the engulfment of apoptotic cells, although with less efficiency than Tim-1 or Tim-4 (Nakayama et al., 2009).

Tim-4 is expressed by macrophages and dendritic cells in the spleen, lymph nodes, thymus, and tonsils (Shakhov et al., 2004), and Tim-3 is expressed in $CD8^+$ dendritic cells in the spleen (Nakayama et al., 2009). These macrophages and dendritic cells are responsible for the engulfment of apoptotic cells and for the presentation of dead cell-associated antigens (Miyake et al., 2007). Tim-1, also called kidney injury molecule 1 (Kim-1), is expressed in kidney epithelial cells after ischemic injury (Ichimura et al., 2008) and in Th2 cells (Umetsu et al., 2005). In the kidney, Tim-1 is likely to be responsible for engulfing the damaged apoptotic or necrotic cell debris generated during ischemic injury, but the role of Tim-1 in Th2 cells is not clear. The Tim family genes are clustered on human chromosome 5q33.2 and mouse chromosome 11B1.1, which is the susceptible gene locus for the development of atopy (allergic hypersensitivity) and asthma (Kuchroo et al., 2003). Whether the newly identified function of Tim-1, Tim-3, and Tim-4 in apoptotic cell engulfment or the originally proposed function of Tim-1 and Tim-4 in the costimulation of T cells (Kuchroo et al., 2003) is responsible for this phenotype remains to be studied.

Park et al. (2007) report that brain-specific angiogenesis inhibitor 1 (BAI1), a member of the secretin/vasoactive intestinal polypeptide (VIP) receptor family with 7-transmembrane regions, is another potential phosphatidylserine receptor for apoptotic cells. BAI1 binds via thrombospondin type 1 repeats (TSPs) to phosphatidylserine, as well as to cardiolipin and other phospholipids. Its cytoplasmic region can interact with the signal transducer ELMO (see below) (Park et al., 2007). However, BAI1's possible function as a phosphatidylserine receptor for apoptotic cells seems to conflict with its neuron-specific expression in the brain (Mori et al., 2002). Another candidate phosphatidylserine receptor is stabilin-2, also called HARE (hyaluronic acid receptor for endocytosis), a type I membrane protein that carries a large extracellular region with seven fasciclin domains and fifteen EGF-like domains (Park et al., 2008). It is expressed by the sinusoidal endothelial cells of the spleen, lymph nodes, and bone marrow (Nonaka et al., 2007) and functions as a receptor for hyaluronic acids and heparin to regulate blood viscosity (Harris et al., 2008). How stabilin-2 accomplishes two jobs, as a phosphatidylserine receptor for apoptotic cells and as a scavenger receptor for hyaluronic acids, would be an interesting topic for study.

Signaling Pathways for Engulfment

Genetic analyses in *C. elegans* identified seven genes that mediate the recognition and engulfment of apoptotic cells in two parallel and partially redundant signaling pathways (the CED-1/-6/-7 and CED-2/-5/-10/-12 pathways) (Table 1) (Reddien and Horvitz, 2004). CED-1 is a transmembrane receptor that has multiple EGF-like domains in its extracellular region; it has high homology with mammalian multiple EGF-like-domains 10 (MEGF10) (Hamon et al., 2006) and may recognize phosphatidylserine on apoptotic cells (Venegas and Zhou, 2007). CED-6 is an ortholog of mammalian GULP (PTB [phosphotyrosine-binding] domain-containing engulfment adaptor protein) and binds to the intracellular domain of CED-1 (Su et al., 2002). CED-7 is homologous to the ABC transporters that actively transport a variety of substances across the plasma membrane and was originally suggested to be responsible for exposing the "eat me" signal on apoptotic cells. However, the ABC transporter CED-7 interacts with MEGF10 (CED-1) (Hamon et al., 2006), indicating that it functions in the engulfment process in phagocytes.

CED-2, -5, -10, and -12 correspond to mammalian CrkII, Dock180, Rac1, and ELMO1, respectively. CED-2/CrkII associates with CED-5/Dock180, a guanine-nucleotide exchange

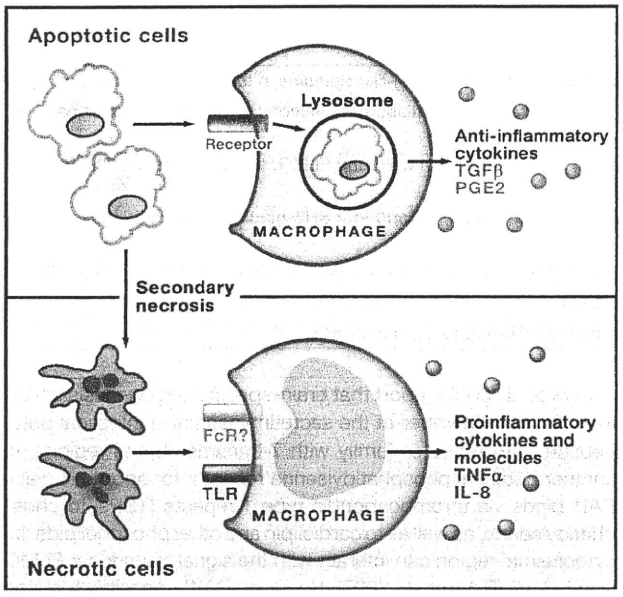

Figure 4. The Engulfment of Apoptotic versus Necrotic Cells
Macrophages engulfing apoptotic cells produce transforming growth factor β (TGFβ) and prostaglandin E2 (PGE2), which function as anti-inflammatory agents to inhibit the further recruitment of macrophages. When dead cells undergo secondary necrosis, the necrotic cells may activate macrophages through Fc receptor (FcR) and Toll-like receptors (TLRs) to produce inflammatory cytokines, such as tumor necrosis factor α (TNFα) and interleukin 8 (IL-8), which act to recruit more macrophages.

factor for CED-10/Rac1, and this interaction is positively regulated by CED-12/ELMO1 (Côté and Vuori, 2007). This pathway regulates actin polymerization and is involved not only in apoptotic-cell engulfment (Figure 3) but also in cell migration, neurite growth, and myoblast fusion. Integrin family members may act upstream of this pathway, but how apoptotic cells activate this pathway remains to be determined.

The engulfment of apoptotic cells is regulated by Rho family GTPases (Rac1, RhoA, Rab5, etc.) (Nakaya et al., 2006) and can be monitored at the molecular level by imaging using an actin-green fluorescent protein (GFP) fusion protein (Nakaya et al., 2008). This type of analysis indicates that the engulfment of apoptotic cells appears to occur at a limited number of portals in the phagocyte lamellipodia. A fluorescence resonance energy transfer (FRET) analysis for Rac1 indicates that the activation and deactivation of Rac1, controlled by "engulfment synapses," must be regulated with specific timing for the efficient engulfment of apoptotic cells. That is, when a phagocyte starts to engulf an apoptotic cell, activated Rac1 and integrin are recruited to the portal and induce the formation of phagocytic cups consisting of an actin patch. As soon as the dead cell sinks into the phagocyte through one of these cups, Rac1 is inactivated and the actin is depolymerized. Subsequently, Rab5 regulates the transfer of the dead-cell cargoes into lysosomes (Kitano et al., 2008).

The uptake of apoptotic cells by phagocytes induces the expression of transforming growth factor β (TGFβ) and IL-10 (Fadok et al., 2001) (Figure 4), which may inhibit the further recruitment of macrophages to the dying cells. On the other hand, if the dead cells persist in tissues, either because of impaired engulfment or because the number of apoptotic cells overwhelms the capacity of the phagocytes, the apoptotic cells undergo necrosis. When necrotic cells interact with or are engulfed by macrophages, the macrophages produce inflammatory cytokines (Fadok et al., 2001), which may recruit more macrophages as reinforcements. The activation of different cytokine genes upon their engulfment of apoptotic and necrotic cells suggests that the signal transduction pathways induced by these dead cells are different.

Autoimmune Disease Caused by the Inefficient Engulfment of Dead Cells

Systemic Lupus Erythematosus is a chronic autoimmune disease that causes a broad spectrum of clinical manifestations affecting the skin, kidney, lungs, blood vessels, and nervous system (D'Cruz et al., 2007). Patients with SLE have autoantibodies in their sera against nuclear components (anti-ribonucleoprotein and anti-DNA antibodies) and sometimes exhibit circulating DNA or nucleosomes (Rumore and Steinman, 1990). As unengulfed apoptotic cells are present in the germinal centers of the lymph nodes of some SLE patients and macrophages from these patients often show a reduced ability to engulf apoptotic cells, a deficiency in the clearance of apoptotic cells is proposed to be one of the causes of SLE (Gaipl et al., 2006).

MFG-E8-deficient female mice, particularly of the B6/129-mixed background, develop an age-dependent SLE type of autoimmune disease (Hanayama et al., 2004). These mice produce high concentrations of anti-double-stranded DNA and anti-nuclear antibodies and suffer from glomerular nephritis. When MFG-E8-deficient mice are immunized with keyhole limpet hemocyanin (KLH) to activate B lymphocytes, many apoptotic cells are left unengulfed on the tingible-body macrophages in the germinal centers, confirming that MFG-E8 has a nonredundant role in vivo in the engulfment of apoptotic cells by the tingible-body macrophages. It is likely that the unengulfed dead cells in MFG-E8-deficient mice undergo a secondary necrosis and release cellular components that activate the immune system to produce autoantibodies (Figure 5A). Like Fas-deficient lpr mice, in which autoreactive B cells are activated in a T cell-independent but Toll-like receptor (TLR)- and B cell receptor (BCR)-dependent mechanism (Herlands et al., 2008), the released cellular components may activate autoreactive B cells in a BCR- and TLR-dependent manner. This activation of autoreactive B cells may be further enhanced by cytokines produced by macrophages in response to stimulation by the necrotic cells. In any case, the MFG-E8-deficient mice provide a good model system for studying the molecular mechanisms by which endogenous cellular components activate the immune system extracellularly.

As described above, apoptotic cells are rapidly recognized and engulfed by macrophages at the early stage of their death process, mostly in a phosphatidylserine-dependent manner. On the other hand, how necrotic cells are recognized and engulfed by macrophages is not well elucidated. One likely system for clearing necrotic cells is the complement system (Trouw et al., 2008). C1q binds to dead cells at the later stages of apoptosis in an IgM-dependent manner (Ogden et al., 2005), and one of the signals on the dead cells for IgM-binding is lysophosphatidylcholine (Kim et al., 2002). Notably, in humans, almost all individuals deficient in

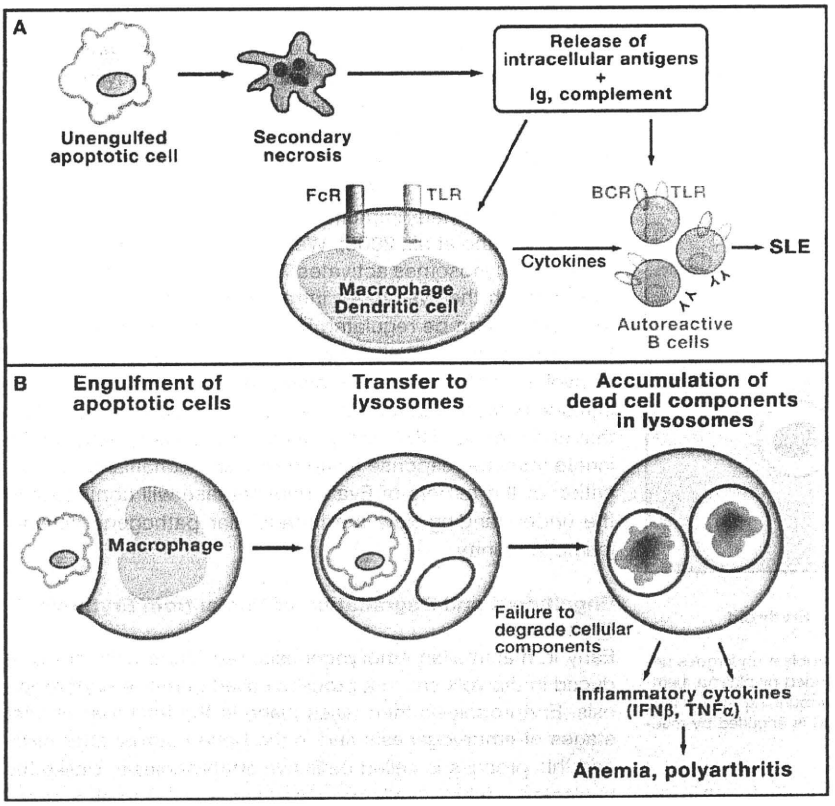

Figure 5. Immune System Activation by the Defective Engulfment of Apoptotic Cells

(A) Extracellular activation. If apoptotic cells are not swiftly engulfed, they undergo secondary necrosis, in which the plasma membrane is disintegrated, and the cellular components are released. Immunoglobulins and complement proteins bind to these cellular components and activate macrophages and B lymphocytes. In addition to FcR and B cell receptors (BCRs), Toll-like receptors (TLRs) appear to be involved in recognizing the cellular components and activating macrophages and B cells. The activated macrophages produce cytokines that will stimulate B cells to produce autoantibodies.

(B) Intracellular activation. After being engulfed by macrophages, dead cells are transferred to lysosomes and degraded. If the degradation does not occur properly, dead cell components accumulate in the lysosomes, leading to the intracellular activation of the innate immune system to produce proinflammatory cytokines such as interferon β (IFNβ) and tumor necrosis factor α (TNFα).

the *C1q* gene develop severe SLE (Botto and Walport, 2002). In C1q-deficient mice, unengulfed dead cells persist in the glomeruli of the kidneys, and the mice develop an SLE-like phenotype; this is particularly evident in the MRL/MP strain, which has a defect in the clearance of apoptotic cells (Potter et al., 2003). In this regard, the C1q-mediated engulfment may be a backup system for clearing dead cells, and it may be informative to cross C1q-deficient mice with MFG-E8-deficient mice.

Degradation of Apoptotic Cells in Macrophages

Activation of the Innate Immunity by Undigested DNA Left in Lysosomes

After apoptotic cells are engulfed by phagocytes, all of their components are degraded into amino acids, nucleotides, fatty acids, and monosaccharides in lysosomes. As described above, the chromosomal DNA of the apoptotic cells is degraded cell autonomously into 180 bp nucleosomal units by CAD and then further degraded in the lysosomes of macrophages. The enzyme that degrades the DNA of apoptotic cells in lysosomes is DNase II (Kawane et al., 2003), which functions under acidic conditions (Evans and Aguilera, 2003). DNase II is ubiquitously expressed in various tissues, particularly in macrophages. A lack of DNase II causes the accumulation of 180 bp fragmented DNA in macrophages (Kawane et al., 2001) and activates the macrophages to produce various cytokines. One of the cytokines produced by these macrophages is IFNβ, which is cytotoxic to erythroblasts and lymphocytes (Yoshida et al., 2005b) (Figure 5B).

Lethal Anemia and Polyarthritis Resulting from a Defect in DNA Degradation

Mice lacking DNase II die late in embryogenesis because of severe anemia (Kawane et al., 2001). Many TUNEL-positive erythroblasts can be found in the liver of mouse embryos lacking DNase II, and a deficiency in the *IFN-type I receptor* gene rescues their lethality (Yoshida et al., 2005b), indicating that the erythroblasts are killed by the action of IFNβ. Mice with a double deficiency for DNase II and IFN-type I receptor, or mice in which the *DNase II* gene is deleted after birth via an inducible conditional knockout strategy, develop polyarthritis as they age (Kawane et al., 2006). Their swollen joints show severe synovitis with aggressive pannus formation. The pannus carries osteoclasts at its leading edge, fills the joint cavity, erodes the cartilage, and destroys the bone. As in the joints of human rheumatoid arthritis patients, the genes for inflammatory cytokines (IL-1β, IL-6, and TNFα) are strongly activated in the affected joints. Human patients with rheumatoid arthritis are successfully treated with reagents that antagonize TNFα or IL-6 (Feldmann, 2002; Yokota et al., 2008). Similarly, the administration of an anti-TNFα antibody significantly improves the clinical score for the polyarthritis developed by the *DNase II* null mice (Kawane et al., 2006).

What triggers the rheumatoid arthritis in humans is unknown. In the *DNase II* null mice, macrophages carrying undigested DNA express *TNFα* mRNA (Kawane et al., 2006), and a low, but significant, level of TNFα is found in the serum before the joints show any abnormality. Given that *TNF*-transgenic mice, which constitutively produce a low level of TNFα, develop polyarthritis (Keffer et al., 1991), it is likely that the TNFα produced by the macrophages carrying undigested DNA is responsible for the development of the polyarthritis. Synovial cells respond to TNFα with high sensitivity to produce IL-1β and IL-6, which in turn stimulate the expression of the TNFα gene (Taberner et

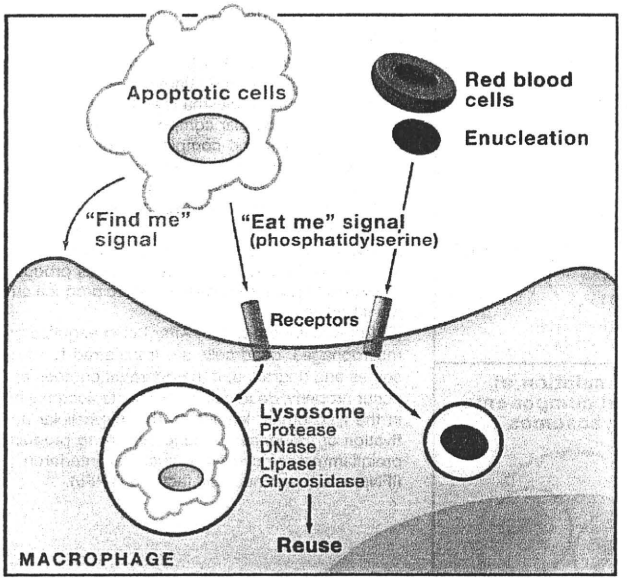

Figure 6. Engulfment of the Nuclei Expelled from Erythroid Precursor Cells

At the final stage of definitive erythropoiesis, an erythroblast undergoes unequal division into a reticulocyte and a nucleus surrounded by plasma membrane. Like apoptotic cells, the plasma membrane surrounding the nucleus exposes phosphatidylserine as an "eat me" signal and is engulfed by macrophages.

al., 2005; Zhang et al., 2004), causing a "cytokine storm" in the joint. This leads to the growth of synovial cells, pannus formation, and the development of polyarthritis (Migita et al., 2001).

The pathologies (anemia and polyarthritis) caused by a deficiency of DNase II are examples of lysosomal storage diseases, which are diseases caused by the inactivation or malfunction of lysosomal enzymes, including proteases, glycosidases, and lipases (Neufeld, 1991). Proteins, polysaccharides, DNA, and RNA of bacterial or viral origin activate the innate immunity to produce various cytokines (Uematsu and Akira, 2007). The results from the *DNase II* null mice indicate that mammalian DNA that accumulates in the lysosomes of macrophages also activates the innate immune response. Other cellular components that escape degradation in the lysosomes may also activate the *TNFα* and *IFNβ* genes. The fact that cytokines are constitutively secreted by macrophages lacking lysosomal acid lipase (Lian et al., 2004), and by fibroblasts derived from patients with Niemann-Pick Disease Type C (Suzuki et al., 2007), an inherited lipid storage disorder, may support this notion. Some patients with rheumatoid arthritis can be cured by bone marrow transplantation (Ikehara, 2002), suggesting that these patients have a defect(s) in bone-marrow-derived cells. Determining whether these patients have lysosomal enzyme defects will be useful for improving their treatment.

Signaling from DNA to Cytokine Gene Expression

Cells that are infected by viruses or bacteria normally produce IFNβ and TNFα (Honda et al., 2006). There are two pathways by which pathogens activate the cytokine genes. In one, TLR recognizes pathogens extracellularly and transduces signals via the adaptor proteins MyD88 and TRIF to activate the transcription factors IFN-regulatory factor (IRF)3/IRF7 and NF-κB, which induce IFNβ and TNFα. In the other pathway, RIG-I/MDA5 recognizes intracellular pathogens and activates IRF3/IRF7 and NF-κB via an adaptor called IPS-1. The expression of the IFNβ and TNFα genes in the macrophages lacking DNase II is not blocked by a deficiency in the TLR system, indicating that the mammalian DNA that accumulates in the lysosomes activates the innate immune system in a TLR-independent manner (Okabe et al., 2005). We recently found that mammalian DNA in lysosomes activates *TNFα* and *IFNβ* gene expression through the system for intracellular pathogens and that this system can be regulated by Janus phosphatases called Eyes absent (Eya) (Okabe et al., 2009). Eya binds to IPS-1 and is involved not only in the mammalian DNA-mediated innate immune reaction but also in the virus-induced one, indicating that endogenous DNA and viruses intracellularly activate the innate immune response using a similar mechanism. Identification of the targets of Eya's phosphatase will contribute to the understanding how the intracellular pathogens activate innate immunity.

Engulfment and Degradation of Nuclei from Erythroid Precursors

Early in mammalian embryogenesis, red blood cells are produced in the yolk sac in a process called primitive erythropoiesis. Erythropoiesis then takes place in the fetal liver at later stages of embryogenesis and in the bone marrow after birth, and this process is called definitive erythropoiesis. Unlike the nucleated erythroid cells produced in the yolk sac, those produced in the fetal liver and bone marrow are enucleated. The definitive erythropoiesis in both the bone marrow and fetal liver takes place in anatomical units called erythroblastic islands. At the center of each island, there is a macrophage that supports the proliferation and differentiation of the erythroid precursor cells (Chasis and Mohandas, 2008). At the final stage of erythropoiesis, the erythroid cells autonomously undergo enucleation, and the expelled nuclei are engulfed by the central macrophage, suggesting that the expelled nuclei also expose an "eat me" signal on their surface (Figure 6).

The engulfment of expelled nuclei by macrophages has been shown to be phosphatidylserine dependent in experiments using nuclei collected from cultured erythroid precursor cells that spontaneously undergo enucleation (Yoshida et al., 2005a). Immediately after a nucleus is separated from its reticulocyte, phosphatidylserine is exposed on the outer leaflet of the plasma membrane surrounding the nucleus. It is likely that the plasma membrane cannot maintain its integrity because of a lack of ATP, because once separated from the reticulocyte, the nucleus loses its sources of new ATP (mitochondria and glycolysis). It is not yet known what molecules in the macrophages of the fetal liver and bone marrow are involved in recognizing the phosphatidylserine on the nuclei and engulfing them.

Every day, 2×10^{11} new red blood cells are produced in a human adult, meaning that this number of nuclei needs to be phagocytosed. This is at least ten times the number of dead cells. If nuclei, which are highly immunogenic, are released into the circulation because of inefficient engulfment, they will activate the immune system. In DNase II-deficient mice,